UNIVERSIDADE DE SÃO PAULO

ESCOLA DE ENGENHARIA DE SÃO CARLOS

DEPARTAMENTO DE ENGENHARIA ELÉTRICA

PROGRAMA DE PÓS-GRADUAÇÃO EM ENGENHARIA ELÉTRICA

Proposal of a New Approach for BER Evaluation of Multirate, Multiservice OCDMA Systems

AUTHOR: Thiago Roberto Raddo

SUPERVISOR: Dr. Ben-Hur Viana Borges

Dissertation submitted to the São Carlos School of Engineering as part of the requirements to obtain the degree of Master of Science, Electrical Engineering Program, with emphasis on Telecommunications.

São Carlos – SP

2012

Ficha catalográfica preparada pelo
Serviço de Biblioteca – EESC/USP

Raddo, Thiago Roberto
R125p Proposta de uma nova abordagem para o cálculo da BER de sistemas OCDMA de múltiplas taxas e mutiserviços = Proposal of a new approach for BER evaluation of multirate, multiservice OCDMA systems / Thiago Roberto Raddo ; orientador Ben-Hur Viana Borges. -- São Carlos, 2012.

Dissertação (Mestrado - Programa de Pós-Graduação em Engenharia Elétrica e Área de Concentração em Telecomunicações) -- Escola de Engenharia de São Carlos da Universidade de São Paulo.

1. Acesso múltiplo por divisão de código óptico (OCDMA). 2. Taxa de erro de bit (BER). 3. OOC de múltiplas ponderações e múltiplos comprimentos. 4. Salto rápido em frequência óptica. 5. Sistemas de múltiplas taxas e multiserviços. 6. Distribuição poissoniana, Gaussiana e Binomial. 7. MAI. 8. Sistemas incoerentes. 9. Rede óptica passiva (PON). I. Título.

UNIVERSIDADE DE SÃO PAULO

ESCOLA DE ENGENHARIA DE SÃO CARLOS

DEPARTAMENTO DE ENGENHARIA ELÉTRICA

PROGRAMA DE PÓS-GRADUAÇÃO EM ENGENHARIA ELÉTRICA

Proposal of a New Approach for BER Evaluation of Multirate, Multiservice OCDMA Systems

AUTHOR: Thiago Roberto Raddo

SUPERVISOR: Dr. Ben-Hur Viana Borges

Dissertation submitted to the São Carlos School of Engineering as part of the requirements to obtain the degree of Master of Science, Electrical Engineering Program, with emphasis on Telecommunications.

Trata-se da versão corrigida da dissertação. A versão original se encontra disponível na EESC/USP que aloja o Programa de Pós-Graduação de Engenharia Elétrica.

FOLHA DE JULGAMENTO

Candidato: Tecnólogo **THIAGO ROBERTO RADDO.**

Título da dissertação: "Proposal of a new approach for BER evaluation of multirate, multiservice OCDMA systems".

Data da defesa: 24/08/2012

Comissão Julgadora:	**Resultado:**
Prof. Associado **Ben-Hur Viana Borges (Orientador)** (Escola de Engenharia de São Carlos/EESC)	APROVADO
Prof. Dr. **Gustavo Fraidenraich** (Universidade Estadual de Campinas/UNICAMP)	APROVADO
Prof. Dr. **Marcelo Luís Francisco Abbade** (Pontifícia Universidade Católica de Campinas/PUC-Campinas)	APROVADO

Coordenador do Programa de Pós-Graduação em Engenharia Elétrica e Presidente da Comissão de Pós-Graduação:
Prof. Titular **Denis Vinicius Coury**

ACKNOWLEDGEMENTS

Firstly, I would like to thank God for everything in life. I would like to thank my parents, Roberto Raddo and Abgail Raddo, for their constant support, love, encouragement, and total comprehension.

I would like to thank my supervisor, Dr. Ben-Hur Viana Borges, for his continuous guidance, helpfulness, confidence, advices, and for giving me the opportunity to accomplish this research.

I would also like to express my gratitude to my friends:

Alex, Arturo, Clenilson, Daniel Marchesi, Daniel Mazulquim, Getúlio, Helvécio, Israel, Larissa, Leone, Lídia, Luiz, Marcel, Mariana, Pedro, Rafael, Thiago Campos, Thiago Franco, Tudela, Ulysses, Valdemir, Willian, and Yang.

I owe special thanks to Anderson L. Sanches for all important discussions about OCDMA.

Finally, I also want to thank the research sponsor, CAPES, for the financial support.

To my beloved grandparents, Alcides and Mercedes.

ABSTRACT

RADDO, T. R. (2012). PROPOSAL OF A NEW APPROACH FOR BER EVALUATION OF MULTIRATE, MULTISERVICE OCDMA SYSTEMS. RESEARCH MASTER – SÃO CARLOS SCHOOL OF ENGINEERING, UNIVERSITY OF SÃO PAULO, SÃO CARLOS, 2012.

The continuous evolution of the optical communication technology in the last few years has allowed the growing users' demand for higher bandwidth to be satisfactorily attended. This new demand is mainly attributed to the growing popularity of bandwidth-intensive networking applications, such as Internet protocol television (IPTV), high-definition television (HDTV), e-learning, e-health, super high-definition (SHD) class digital movies, and e-culture based on 3-D full-HD video. These applications will eventually require differentiated service types and diversified data rates. As a result, capability of supporting differentiated-quality of service (QoS) and multirate transmission are becoming a challenge for future optical networks.

Among many multiplexing techniques, optical code-division multiple-access (OCDMA) constitutes a potential candidate for next generation optical networks, particularly due to features like asynchronous operation, simplified network control, easy addition of new users, and possibility of differentiated-QoS at the physical layer. The performance of this access technique is mainly limited by multiple-access interference (MAI).

Although in multirate, multiservice OCDMA systems MAI is considered to be binomially distributed, others probability distributions for the MAI analyzes and consequently the bit error rate (BER) have been used as an approximation. In this context, this dissertation proposes a new formalism to evaluate the BER performance of 1-D and 2-D multirate, multiservice OCDMA systems considering MAI as binomially distributed, resulting in a more accurate BER expression. Also, the proposed approach does not require knowledge *a priori* of the generated code sequences themselves, which means that the system performance analysis is achieved more easily using only the code parameters.

Furthermore, a multirate OCDMA system employing 1-D optical orthogonal code (OOC) and 2-D optical fast frequency hopping (OFFH) codes is also investigated. A performance comparison in terms of BER for the OOC-based system assuming both Poisson and binomial distribution for the MAI is investigated. A further comparison of an OFFH-

based multirate system assuming both gaussian and binomial distribution for the MAI is also analyzed. It is shown that BER performance in multirate scenarios can be overestimated or underestimated by many orders of magnitude depending on the assumed distribution for the MAI and on the number of simultaneous users. Moreover, it is presented for the first time a hybrid OCDM/WDM optical packet switch capable of supporting multirate and differentiated-QoS transmission. The architecture of the proposed multirate switch and its performance in terms of packet loss probability are also presented.

Finally, it is shown that using a gaussian or Poisson distribution for the MAI might not be appropriate for a reliable BER estimate, since they are not acceptable approximations to assess the performance of multirate, multiservice systems with good accuracy.

Key-words: optical code-division multiple-access (OCDMA), bit error rate (BER), multi-weight multi-length OOC, optical FFH, multirate multiclass multiservice systems, Poisson, gaussian, binomial distribution, MAI, incoherent systems, passive optical network (PON).

RESUMO

RADDO, T. R. (2012). PROPOSTA DE UMA NOVA ABORDAGEM PARA O CÁLCULO DA BER DE SISTEMAS OCDMA DE MÚLTIPLAS TAXAS E MULTISERVIÇOS. MESTRADO – ESCOLA DE ENGENHARIA DE SÃO CARLOS, UNIVERSIDADE DE SÃO PAULO, SÃO CARLOS, 2012.

A contínua evolução da tecnologia de comunicações ópticas observada nos últimos anos vem possibilitando atender a crescente demanda dos usuários por maior largura de banda. Esta nova demanda é atribuída principalmente à popularidade crescente de aplicações de banda larga, tais como TV por protocolo de Internet (IPTV), televisão de alta definição (HDTV), ensino online, e-saúde, filmes digitais de super alta definição (SHD) e e-cultura baseado em vídeo 3-D full-HD. Esta vasta gama de aplicações acabará por necessitar de tipos de serviços diferenciados e taxas de transmissão de dados diversificadas. Como resultado, capacidades de suportar diferenciamento de qualidade de serviço (QoS) e transmissão de múltiplas taxas estão se tornando um desafio para as redes ópticas futuras.

Dentre muitas técnicas de multiplexação existentes, OCDMA constitui-se em um candidato potencial para as redes ópticas de próxima geração, particularmente devido a características como operação assíncrona, controle de rede simplificada, fácil adição de novos usuários, e também possibilidade de QoS diferenciado na camada física. O desempenho desta técnica de acesso múltiplo é limitado principalmente por interferência múltipla de acesso (MAI).

Embora em sistemas OCDMA de múltiplas taxas e multiserviços a MAI deva ser considerada binomialmente distribuída, outras distribuições de probabilidade para a análise da MAI e, consequentemente, da BER têm sido utilizadas como uma aproximação. Neste contexto, este trabalho propõe um novo formalismo para avaliar o desempenho da BER de sistemas OCDMA 1-D e 2-D de múltiplas taxas e multisserviços considerando a MAI como binomialmente distribuída, o que resulta em uma expressão mais precisa para a BER. Além disso, o método proposto neste trabalho não requer conhecimento, *a priori*, das sequências de códigos geradas, o que significa que a análise do desempenho do sistema é obtida mais facilmente utilizando apenas os parâmetros do código.

Um sistema OCDMA de múltiplas taxas empregando códigos 1-D OOC e 2-D OFFH será também investigado. Uma comparação do desempenho em termos de BER para o sistema baseado em OOC supondo tanto a distribuição de Poisson quanto a binomial para a

MAI é investigada. De forma análoga, uma comparação para o sistema de múltiplas taxas baseado em OFFH supondo desta vez tanto a distribuição gaussiana quanto a binomial para a MAI também é analisada. É mostrado que a BER em cenários de múltiplas taxas pode ser superestimada ou subestimada em várias ordens de grandeza, dependendo da distribuição suposta para a MAI e do número de usuários simultâneos no sistema. Além disso, é apresentado pela primeira vez um switch óptico híbrido de pacotes OCDM/WDM capaz de prover transmissões de múltiplas taxas e serviços diferenciados. A arquitetura do switch proposto e seu desempenho em termos de probabilidade de perda de pacotes também são apresentados.

Finalmente, é mostrado que o uso da distribuição gaussiana ou poissoniana para a MAI pode não ser apropriado para uma estimativa confiável de BER, uma vez que não são aproximações aceitáveis para avaliar o desempenho de sistemas de múltiplas taxas e multiserviços com boa precisão.

Palavras-chave: acesso múltiplo por divisão de código óptico (OCDMA), taxa de erro de bit (BER), OOC de múltiplas ponderações e múltiplos comprimentos, salto rápido na frequência óptica, sistemas de múltiplas taxas e multiserviços, distribuição poissoniana, gaussiana e binomial, MAI, sistemas incoerentes, rede óptica passiva (PON).

CONTENTS

LIST OF FIGURES

LIST OF SYMBOLS

T_b	Bit period
T_j	Bit period of *j*th user class
T_c	Chip period
L	Code length
W	Code weight
L_j	Code length of *j*th user class in the system
L_J	Code length of last user class in the system
U	Total number of users
U_j	Total number of users in class *j*
$S_{u,j}(t,f)$	Transmitted signal of the *u*th user in the *j*th class
$b_{u,j}(t)$	Baseband signal of the *u*th user in the *j*th class
$C_{u,j}(t,f)$	Hopping pattern of the *u*th user in the *j*th class
$r(t,f)$	Broadcasted received signal
$b_{1,j'}$	Reference bit of the desired user
$I^{1,j'}_{(j=j',u)}$	MAI from users of same code lengths that desired user
$I^{1,j'}_{(j>j',u)}$	MAI from users with code lengths longer than the desired user's code length
$I^{1,j'}_{(j<j',u)}$	MAI from users with code lengths shorter than the desired user's code length
$I_{j'}$	Total MAI of the system generated on the desired class
j'	The desired user class
$W_{j'}$	Code weight of the users' desired class
W_j	Code weight of the users' interfering class
$M_{I_{j'}}(t)$	Moment-generating function of total interference
$p_{jj'}$	Probability of hit between a code from class *j* and a code from class *j'*
$p_{j'j'}$	Probability of hit between a code from class *j'* and a code from class *j'*
F	Total number of available wavelengths
η	Mean of the MAI
σ^2	Variance of the MAI
$M'_{I_{j'}}(0)$	First moment of the moment-generating function
$M''_{I_{j'}}(0)$	Second moment of the moment-generating function
$\mathcal{P}$	Probability of interference of a multirate, multiservice system

$P(error\|0)$	Probability of false alarm
$P(error\|1)$	Probability of false dismissal
$BER(j')$	Bit error rate of the desired j' class
μ	Threshold level of the decision device
μ_{opt}	Optimum threshold level of the decision device
$P(Z \geq \mu \| b_{1,j'} = 0)$	Probability that a bit "0" is transmitted and Z reaches or exceeds the detection threshold
$P(Z < \mu \| b_{1,j'} = 1)$	Probability that a bit "1" is transmitted and Z does not exceed the detection threshold
$Q(\cdot)$	*Q*-function
s(t)	Code Sequence signature
f(t)	Code mask
r(t)	Signal after correlation between a specific code and its mask
$Z_{x,x}$	Autocorrelation function
$Z_{x,y}$	Cross-correlation function
λ_a	Out-of-phase autocorrelation peak
λ_c	Cross-correlation peak
λ_F	Last available wavelengths in the OFFH system
n_{eff}	Effective index
L_s	Spacing between two adjacent Bragg gratings
c	Speed of light
N_j	Number of interfering users in relation to the desired user
B	Data rate transmission

Chapter 4

λ_m	*m*th wavelength from *M* available wavelengths
DA_C_j	Decoder array that includes all decoders of users class *j*
EA_C_J	Encoder array that includes all encoders of users class *j*
SF_A	Switching Fabric
SF_i	*i*th Switching Fabric
WC_r	*r*th Wavelength converter
WC_R	Total number of available wavelength converters
F_j	Total number of packets in class *j*
F	Total number of packets in the system
C	Total code sets available
C_j	Code set of the *j*th class
C_J	The last available code set in the system
$c_{f,j}$	The fth codeword of the jth class
$c_{F_j,j}$	The last available codeword of the *j*th class
$(i, \lambda_m, c_{f,j})$	Triplet that identify the input (output) fiber, and the respective wavelength and codeword.

$\Lambda_{i,m,j}$	The set of all available output channels (codewords) in the *i*th output fiber, *m*th wavelength, and *j*th class.
$I_{i,m,j}$	Set of packets arrived in *i*th output fiber, forwarded to *j*th class in *m*th wavelength.
I_i	Set of left packets from $I_{i,m,j}$
Λ_i	Set of left output channels from $\Lambda_{i,m,j}$
b	A random chosen packet
H	Packet length in bits
p	Offered traffic

LIST OF ACRONYMS

AON	Active Optical Network
APD	Avalanche Photodiode
ASK	Amplitude Shift Keying
BER	Bit Error Rate
BPSK	Binary-Phase-Shift-Keying
CDMA	Code-Division Multiple-Access
CLT	Central Limit Theorem
DS	Direct-Sequence
FBG	Fiber Bragg Grating
FE	Frequency Encoded
FEC	Forward Error Correction
FFH	Fast Frequency Hopping
FH	Frequency-Hopping
FTTB	Fiber To The Building
FTTC	Fiber To The Curb
FTTH	Fiber To The Home
FTTx	Fiber To The x
HDTV	High-Definition Television
IM-DD	Intensity-Modulation Direct-Detection
IPTV	Internet Protocol Television
LED	Light-Emitting Diode
MAI	Multiple-Access Interference
MBGs	Multiple Bragg Gratings
MWML-OOC	Multi-Weight Multi-Length OOC
MWOOC	Multiple-Wavelength Optical Orthogonal Code
OCDM	Optical Code-Division Multiplexing
OCDMA	Optical Code-Division Multiple-Access

OCDM/WDM	Optical Code-Division Multiplexing/Wavelength-Division Multiplexing
OCFHC/OOC	One-Coincidence Frequency-Hopping Code/Optical Orthogonal Code
ODLs	Optical Delay Lines
OFFH	Optical Fast Frequency Hopping
OOC	Optical Orthogonal Code
OOK	On-Off Keying
OPS	Optical Packet Switch
PC/OOC	Prime Code/Optical Orthogonal Code
PDF	Probability Density Function
PON	Passive Optical Network
PLP	Packet Loss Probability
QoE	Quality of Experience
QoS	Quality of Service
RS	Reed-Solomon
RTT	Round-Time Trip
SHD	Super High-Definition
TDM	Time-Division Multiplexing
TDMA	Time-Division Multiple-Access
TDM/OCDMA	Time-Division Multiplexing/Optical Code-Division Multiple-Access
VoD	Video-on-Demand
WDM	Wavelength-Division Multiplexing
WDMA	Wavelength-Division Multiple -Access
WDM/OCDMA	Wavelength-Division Multiplexing/Optical Code-Division Multiple-Access
1-D	One-Dimensional
2-D	Two-Dimensional
3-D	Three-Dimensional

LIST OF PUBLICATIONS

P1. **T. R. RADDO,** A. L. SANCHES, J. V. dos REIS Jr., and B.-H. V. BORGES, "A New Approach for Evaluating the BER of a Multirate, Multiclass OFFH-CDMA System," *IEEE Communications Letters*, vol. 16, no. 2, pp. 259-261, February, 2012.

P2. **T. R. RADDO,** A. L. SANCHES, J. V. dos REIS Jr., and B.-H. V. BORGES," Influence of the MAI Distribution over the BER Evaluation in a Multirate, Multiclass OOC-OCDMA System," in *Access Networks and In-house Communications, ANIC* 2011, OSA, Toronto, Canada, June 2011.

P3. **T. R. RADDO,** A. L. SANCHES, J. V. dos REIS Jr., and B.-H. V. BORGES, "Performance Evaluation of a Multirate, Multiclass OCDM/WDM Optical Packet Switch," in *IEEE International Microwave and Optoelectronics Conference, IMOC* 2011, Natal, Brazil, November 2011.

P4. L. GALDINO, **T. R. RADDO,** A. L. SANCHES, L. H. BONANI, and E. MOSCHIM," Performance Comparison of Hybrid 1-D WDM/OCDMA and 2-D OCDMA Towards Future Access Network Migration Scenario," in *IEEE International Conference on Transparent Optical Networks, ICTON* 2012, Coventry, England, July 2012.

CHAPTER 1

INTRODUCTION

During the last few years, optical communication technology has been evolving continuously in order to meet the users' demands for higher bandwidth. The explosive growth of social networking and video-sharing websites indicate that end-user's demand for high-bandwidth Internet services is at an all-time high. This new demand is also mainly attributed to a growing list of bandwidth-intensive networking applications, such as: Internet protocol television (IPTV), video conferencing, high-definition television (HDTV), interactive distance learning (also referred as e-learning), e-health, telemedicine, super high-definition (SHD) class digital movies, e-culture based on 3-D full-HD video, online movie rental, video-on-demand (VoD), multiplayer on-line games, and also triple-play services (voice, video and data traffic in a single subscription). Combined with the growing demand for HDTV programming and VoD, in which the video stream is delivered to the user when requested, overall end-user bandwidth necessity is expected to grow exponentially. Since these applications will eventually require differentiated service types and diversified data rates, telecom service providers are expected to deliver a far richer range of services than ever before. As a consequence, capability of supporting differentiated-quality of service (QoS) and multirate transmission are becoming a challenge for future optical networks [1]-[8].

It has long been realized that the Internet has been developing rapidly with the ultimate goal of providing people with easy and fast access to any desired information from any part of the world. Furthermore, successful multi-play[1] deployment is offering end-users an unprecedented opportunity for bundled broadband Internet access subscription, digital TV, landline telephone and mobile phone subscriptions. Nevertheless, telecommunication service providers need to continually evolve their existing networks to withstand the rigors of bandwidth-intensive multi-play applications.

[1] Multi-play is a marketing term describing the provision of different telecommunication services, such as broadband Internet access, digital TV, a landline telephone subscription, and a mobile phone subscription.

The deployment of broadband access networks that bring optical fiber near or very close to the customer premises, known as fiber to the x (FTTx) [9]-[12], might be part of this solution. FTTx is a generic term used to describe network architectures of high performance transmission based on optical technology. In order to service providers successfully deliver this huge demand of multi-play services over FTTx they must be prepared to provide services more efficiently and economically to satisfy end-users quality of experience (QoE) expectations in an increasingly sophisticated and competitive market. Telecommunications service providers are therefore looking towards new multiservice, multirate access networks architectures aiming not only at surviving but also at taking the leadership in this competitive market.

Other FTTx solution-based variants are fiber to the building (FTTB), where the final optical fiber equipment is installed in a building; fiber to the curb (FTTC), where the optical fiber cable is directly installed in a street cabinet normally near homes or business places; and finally fiber to the home (FTTH), where the optical fiber is installed at the home premises, such as on the outside wall of a home. Currently, FTTx encompasses the entire set of access network architectures that are enabling telecom companies to bring broadband services to the end-user premises.

Generally, optical access networks can be classified into two categories depending on the components involved in its particular technology, namely [9], [13]-[15]: active optical network (AON) and passive optical network (PON). The former employs active components that require electrical power like amplifiers and switches. The latter, on the other hand, employs only passive components in the signal's path from source to destination, like optical splitters and couplers. PON is probably the most attractive technology for access networks, since it is a promising cost-effective solution to deliver a vast amount of data to end-users [16], [17]-[18].

Since the first proposals of access networks various multiplexing techniques have been investigated. The three most popular techniques are shown in Figure 1.1, namely, time-division multiple access (TDMA) [11], [19], wavelength-division multiple access (WDMA) [11], [19], [20] and optical code-division multiple access (OCDMA) [21]-[25]. In TDMA, each user transmits both sequentially and in its own time interval, occupying an exclusively pre-assigned time slot as shown in Figure 1.1(a). Note that in this technique the allocation of dedicated pre-assigned time slots does not allow the achievement of statistical multiplexing, which is normally very desirable in the occurrence of bursty data traffic. Hence, due to this

time-sharing, TDMA is very limited in supporting bursty traffic and providing multirate transmission [26]. Nevertheless, a possible way to support multirate transmission in TDMA could be by employing a central controller that dynamically allocates bandwidth to users according to the traffic load. However, the central controller considerably increases the overall complexity of the system. Furthermore, the TDMA implementation requires optical end-to-end synchronization along the communication path. Therefore, it can be easily concluded that TDMA is not the best candidate to support multiple rates and differentiated quality of service transmissions in next generation passive optical access networks.

WDMA, on the other hand, provides dedicated point-to-point connections to each user without any of the concerns associated with multiple users sharing a single downlink transmission channel like in TDMA. In WDMA all users transmit at the same time interval, but in a dedicated assigned wavelength range, as shown in Figure 1.1(b). Thus, each channel occupies a narrow optical bandwidth around a central wavelength. In spite of that, in this technique the smallest bandwidth granularity is a WDMA window which is inadequately coarse, i.e., the window size might be wider than required [27], [28]. Moreover, this technique requires both fine tuning and constant monitoring of the wavelength emitted by each source, and further constant monitoring of the central wavelength of each filter due to crosstalk elimination purposes between distinct wavelengths. As a result, this network configuration is not the most viable technology to support multiple rates and differentiated quality of service transmissions.

Finally, in OCDMA [21]-[25], [29]-[32] all users transmit at the same time interval and over the same available wavelength range, and for each of these users an exclusive code sequence is assigned, Figure 1.1(c). In other words, the network resources are shared among all users to whom unique codes are assigned instead of a time slot like TDMA or a wavelength like WDMA. Thus all users are able to access the network resources at the same time and using the same wavelength range. Moreover, OCDMA not only supports multiple rates and different classes of services at the physical layer, but it is also well suited for bursty data traffic networks. Furthermore, it overcomes the coarse granularity issue of WDMA in an efficient manner reducing it to a subwavelength, i.e., the bandwidth of a single wavelength is shared among many code sequences resulting in several communication channels.

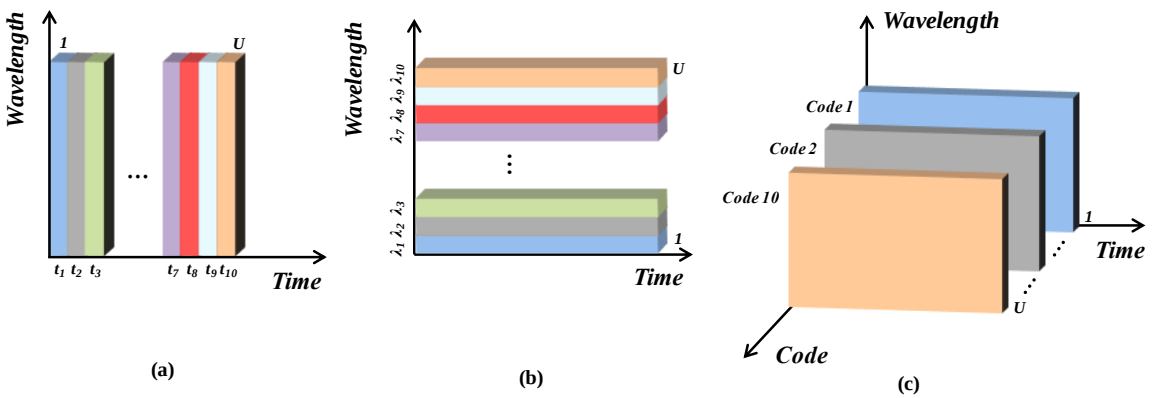

Figure 1.1: Multiple access schemes. U is the total number of users (U = 10 in this example), t is a time slot, and λ is a wavelength. (a) TDMA (the colors distinguish the time slots), each user transmits sequentially in its own time interval, (b) WDMA (the colors distinguish the wavelengths), each user transmits in a range of frequency simultaneously, and (c) OCDMA (the colors distinguish the codes), each user transmits simultaneously using its own code sequence, occupying all frequency range available.

It is worth observing at this point that optical systems based on TDMA and WDMA have fixed channel allocation, which characterize them as deterministic systems. Conversely, optical systems based on OCDMA are characterized as statistical systems since the degradation factor depends on the interfering users present in the system. In other words, the probability of error depends directly on the number of simultaneous users. As can be seen, designing high-capacity networks to handle diverse and bulky data traffic has become a real challenge for next-generation access networks. Nonetheless, OCDMA networks can be more efficiently adapted to multirate and differentiated service transmission, which makes them more appealing for next generation optical access networks. The main advantages of this access technology are [18], [24], [33]:

a) Users can randomly and concurrently access the network, i.e., it provides asynchronous operation;
b) Users can embark or exit without any supervision;
c) Differentiated-QoS and multiple rates transmissions are supported at the physical layer;
d) Capability to secure data transmission using a pseudo-random code signature at the physical layer;

e) Supports bursty traffic;
f) Highly compatible with TDM and WDM;
g) Statistical multiplexing;
h) Flexibility in the code design and high degree of scalability;
i) Simplified and decentralized network control;
j) Low cost and complexity for adding new coming users;
k) Possibility of offering a virtual point-to-point topology as available in WDMA networks;
l) High-speed transmission using all-optical signal processing can be implemented.

These advantages make OCDMA also attractive to be used together with other multiplexing techniques, resulting in a hybrid optical network. For instance, OCDMA with time-division multiplexing (TDM) scheme on the same time slot, giving rise to TDM/OCDMA PON [34]. Another particularly interesting hybrid technology is the WDM/OCDMA PON [35]-[42], in which the bandwidth on one wavelength is divided into small fractions labeled as optical codes and assigned to different transmission channels. This allows a considerable improvement in spectrum efficiency when compared with WDM PON. As pointed out in [35] and [38], the convergence of OCDMA and WDM can be considered as a competitive alternative for future PON.

Commonly, OCDMA networks can be divided into two broad categories [33], depending on how a particular user's code is applied to the optical signal, namely, coherent [43], [44] and incoherent [1], [3], [8], [38]. In coherent OCDMA, the phase of the optical signal is encoded using bipolar codes such as Gold codes and Hadamard. In incoherent OCDMA, the focus of this work, the intensity of the optical signal is encoded using unipolar codes such as fast frequency hopping (FFH) [45] and optical orthogonal code (OOC) [29], [46].

Regardless of the network category, an important issue concerning the performance of OCDMA is the multiple-access interference (MAI). The MAI is directly proportional to the number of simultaneous users on the network, so the higher the number of simultaneous users, the higher the level of MAI generated and the higher will be the desired signal's degradation. Even though other noise sources do exist in the network, MAI is commonly treated as the dominant one [45], [47]-[49]. Therefore, it will also be assumed as the only

degrading factor in this work. For readers interested in OCDMA systems considering other noise sources please refer to [50], [51].

MAI can be briefly defined as the crosstalk among many different users that share a common communication channel. The MAI occurs when many users coexist simultaneously in the channel so that encoded unwanted users' signals generate noise, i.e., make interference on the interest user's code. Normally, the MAI increases the received power and might end up changing a user data bit from zero into one therefore increasing the bit error rate (BER). This noise source severely limits the overall system performance.

Furthermore, the probability density function (PDF) of the MAI is usually approximated as a gaussian one [3], [5], [6], [48], [52]-[55]. A common argument used to justify this approximation is that the number of simultaneous users on a system must be large enough. Thus, MAI will also be large enough providing then an acceptable approximation. This argument, widely adopted in the literature [45], [54], [56], [57], is based on the central limit theorem (CLT) which explains how a probability distribution function can tend to a gaussian distribution.

Briefly, the CLT states that the mean of a sufficiently large number of independent and identically distributed random variables is approximately gaussian distributed. In other words, and into the OCDMA context, the binomially distributed MAI will tend to a gaussian distribution as the number of active users becomes large enough in the system. On the other hand, when the number of users is not large enough, the gaussian approximation statistics becomes highly questionable especially for estimating the system's BER.

Another argument for utilizing a gaussian distribution is that the probability of interference from an interfering user must be as close as possible to 0.5 [55], [58]. If this condition can be satisfied, the approximation will be good and useful enough for replacing the binomial distribution. Unfortunately, this condition is hard to be satisfied in modern OCDMA systems since the probability of interference is normally not as high as established by this rule. Moreover, it is highly desirable that interference should be as low as possible so that the system can perform better and, possibly, accommodate a larger number of users. Again, gaussian approximation is a poor approximation and will not provide a good estimate for the BER of the system, independently of employing code families such as FFH [45] or OOC [29].

The originally proposed OOC [29], [30], [46] was based on equal code weights and code lengths with the assumption of providing equal data rate, i.e., single rate transmission

and equal error rate, i.e., single service transmission. The first multirate OCDMA approach was based on OOC and was limited to two rates only [3]. In this system, the multirate transmission was achieved by varying the spreading factor while maintaining a constant spread bandwidth, which corresponds to vary the code length. Note that varying the code length will eventually change the bit duration. The code set employed in the system had maximum out-of-phase autocorrelation and cross-correlation values bound by three. Since this code set does not have good correlation properties, the system presented high error probability limiting drastically the number of accommodated users in the system. Furthermore, a gaussian distribution for the MAI was assumed in the system performance evaluation.

Tarhuni and Korhonen in [52], introduced a strict multi-weight multi-length OOC (MWML-OOC) OCDMA system. The different code lengths were designed to support data rate differentiation, and the different code weights were designed to support service differentiation. The performance of the system was evaluated based on the assumption that the binomially distributed OOC interference is approximated by a gaussian distribution. As mentioned earlier, this approximation is valid only if the number of users is large enough and the probability of hit from an interfering user is close to 0.5. This assumption, therefore, is no longer accurate in OOC with long code lengths and low code weights.

Beyranvand et al. [1] have investigated a multirate, differentiated-QoS OCDMA system based on multilevel signaling and multistage receiver. The authors proposed a new approach to construct MWML-OOC with any value of correlation property to increase the number of available codes with emphasis on one-dimensional (1-D) OCDMA systems. Ghaffari and Salehi [47] have introduced a novel signaling method and receiver structure based on advanced binary optical logic gates for OCDMA systems. In this system, users are defined in multiple classes with each class transmitting at different power levels.

In [59], a parallel mapping scheme was proposed in order to achieve multirate transmission. The scheme was based on assigning a proportional number of code sequences according to the user data rate. This limited the system applicability because of the limited number of available codes. In [60], a multirate, multi-QoS OCDMA system using *M*-ary overlapping pulse-position modulation (OPPM) and power controller has been proposed. In this system, the power controller is employed to support multi-QoS while the multiplicity factor is varied in order to support multirate transmission.

Another alternative for obtaining a multirate OCDMA system is to use optical fast frequency hopping (OFFH). This technology was originally proposed for single rate transmission by Fathallah et al. [45], and employed equal code lengths in order to satisfy the code correlation properties, and guarantee equal data rate for all users. The first OFFH-CDMA system approach capable of achieving multiple rates was proposed by Inaty et al. [61]. This formalism, capable of achieving multiple rates through variable processing gain, requires knowledge *a priori* of the corresponding users' code sequences before making any system performance analysis. Unfortunately, the performance analysis of the system in terms of BER was not investigated.

A different configuration of OFFH-CDMA system capable of supporting multirate transmission was proposed in [5]. Differently from the previous approaches, in this system the chip duration is varied while keeping constant the code length. Modifying the chip duration is another alternative to vary the bit period. It was demonstrated that the system can accommodate more users than traditional configurations. The performance analysis of the system was based on the gaussian assumption for the MAI.

Inaty et al. [53] have also introduced a power control algorithm to improve the multirate OFFH-CDMA system capacity. Multirate reconfigurability of the encoder-decoder was achieved by changing the length of the hopping pattern using tunable MBG. In [53], the BER evaluation was based on the assumption that the binomially distributed MAI can be approximated by a gaussian distribution. This approximation restricts the performance analysis of the system as discussed before, and therefore is not accurate in multirate OFFH with low code weight and large number of wavelengths.

Inaty et al. later proposed a transmitter-receiver architecture for multirate OFFH-CDMA system in [7]. When transmitting a data bit “0”, the system assigned to each user a frequency-shifted version of the code employed to transmit data bit “1”. Two code sequences are assigned to each user in the system, one to bit “0” and one (its orthogonal version) to bit “1”. However, in order to evaluate the BER performance of this multirate system, the knowledge *a priori* of the code sequences is required.

Tarhuni et al. [58] provided an expansion and full analyzes of a multirate, multiclass 1-D MWML-OOC OCDMA system. In this system, the binomially distributed MAI was approximated by a Poisson distribution in order to simplify the evaluation of the BER. Although approximating the multiclass MAI by a Poisson distribution might prove useful to simplify the system performance analysis, for many multirate scenarios this approximation

might not be considered acceptable. For instance, evaluating the BER by modeling the MAI as poissonian does not lead to good accuracy performance when considering a multirate OCDMA system based on sparse codes, like the MWML-OOC. Since MWML-OOC codes are classified as very sparse codes with usually both long-length and low-weight properties, the BER will only be considered accurate enough when the number of users is large and probability of interference is very low. Note that the probability of interference is directly related to the code properties (length and weight) in a way that the sparser the codes are, the lower will be the probability of interference and, consequently, the better will be the Poisson approximation. In addition, the mathematical formalism proposed in [58] focused on 1-D OCDMA systems which, unfortunately, cannot be directly employed to evaluate the BER of 2-D OFFH-CDMA systems.

It can be seen from the previous discussions that there are many aspects of BER performance evaluation in multirate, multiservice OCDMA systems that yet must be considered. For instance, a mathematical formalism that can accurately evaluate the BER performance of 2-D OCDMA multirate systems assuming MAI as binomially distributed, and a formalism that requires only the code parameters to be provided and not the users' code sequences themselves.

In this context, this work proposes for the first time, a new formalism to evaluate the BER performance of 1-D and 2-D multirate, multiservice OCDMA systems considering MAI as binomially distributed. Different from other formalisms available in the literature, the derived BER expression, and consequently the whole formalism, allows the system performance evaluation not only when data bit "0" is transmitted, but also when a bit "1" is transmitted. Furthermore, the present formalism can be applied to evaluate the BER of any multi-weight multi-length family of 1-D and 2-D codes with maximum cross-correlation and out-of-phase autocorrelation values bounded by one. Also, the proposed formalism only requires the code parameters to be provided and does not employ the users' code sequences themselves, which makes the system analysis straightforward.

Furthermore, a multirate OCDMA system employing 1-D OOC and 2-D OFFH codes is also analyzed. A performance comparison in terms of BER for the MWML OOC-based system assuming both Poisson and binomial distribution for the MAI is investigated. A further comparison for the OFFH-based system assuming both gaussian and binomial distribution for the MAI is also investigated. It is shown that BER performance in multirate scenarios can be overestimated or underestimated by many orders of magnitude depending on

the assumed distribution for the MAI and on the number of simultaneous users. For multirate scenarios with low number of simultaneous users the assumed MAI distributions i.e., Poisson and gaussian, and consequently the BER, diverge from binomial rather than converge.

This dissertation also presents for the first time the analysis of an optical code-division multiplexing/wavelength-division multiplexing (OCDM/WDM) optical packet switch (OPS) architecture capable of supporting multi-QoS and multirate transmission. This analysis was based on the hybrid bufferless OCDM/WDM OPS single service, single rate switch using coherent Gold optical codes proposed in [62]. The authors investigated the system performance taking into account both MAI and beat noise, and further performance analysis considering the output packet contentions was also considered. In the present work, we extend this analysis a step further and propose an OCDM/WDM OPS architecture capable of supporting multi-QoS and multirate transmission. The main idea is to use MWML-OOC as signature sequence of an OCDM system to achieve diversified services and data rates transmission. In addition, the performance of the OCDM/WDM OPS is evaluated in terms of BER taking into consideration the MAI of the multiservice, multirate system. The proposed multiservice optical switch is extremely interesting from a practical point of view, since it does not require any new optical processing as it basically uses the same technology utilized in single service OCDM/WDM hybrid networks.

This dissertation is organized as follows. Chapter 2 introduces the concept of 1-D and 2-D codings utilized in OCDMA networks, and the operation principle of MAI. Chapter 3 begins with the numerical modeling of multirate OCDMA systems and presents the mathematical formalism for the BER. Also in this chapter is presented the new approach to evaluate the BER of multirate, multiservice OCDMA systems. Chapter 4, in turn, introduces a multirate, multiservice hybrid OCDM/WDM optical packet switch and investigates its performance in terms of BER to evaluate the packet loss probability. The most relevant results on the system performance of multirate systems are presented in Chapter 5. Finally, Chapter 6 presents the final conclusions of this work.

CHAPTER 2

OPTICAL CODING AND MAI IN OCDMA SYSTEMS

OCDMA is classified as a spread spectrum technique, which increases the physical bandwidth of the channel by employing a specific spreading code. Spread spectrum, in general, refers to any system where the bandwidth of the signal transmitted on a channel is greater than the bandwidth required to transmit the original information signal. In this type of system, the baseband signal bandwidth is intentionally spread over a larger bandwidth as illustrated in Figure 2.1. The spreading can be made either by direct-sequence (DS), where the data bits are multiplied by a code sequence and thereby divided into shorter pulses known as chips, or by frequency-hopping (FH), where the data bits are spread among several frequency channels. The use of coding schemes grants OCDMA networks a higher level of data security if compared to other networks technology [63].

The most striking feature of OCDMA is that the users' information is encoded before being sent to the transmitting channel. Furthermore, in OCDMA systems the integrity and security of users' information is secured by means of unique signature codes, i.e., exclusive code sequences assigned to each of these users. Nowadays, much effort has been devoted in the literature to the development of robust optical codes which have the desirable characteristic of orthogonality (code differentiation) and large cardinality (large number of available codes).

Generally, OCDMA systems can be divided into two broad categories depending on the way in which a given user’s code sequence is applied to the optical signal [33] incoherent, where a unipolar code such as OFFH is used with on-off keying (OOK) modulation format (where the coding is based on the optical intensity), and coherent, where a bipolar code such as Gold code is used (in this case the coding shifts the optical phase). Most modulation techniques employed in optical systems are characterized by the manipulation of the signal intensity.

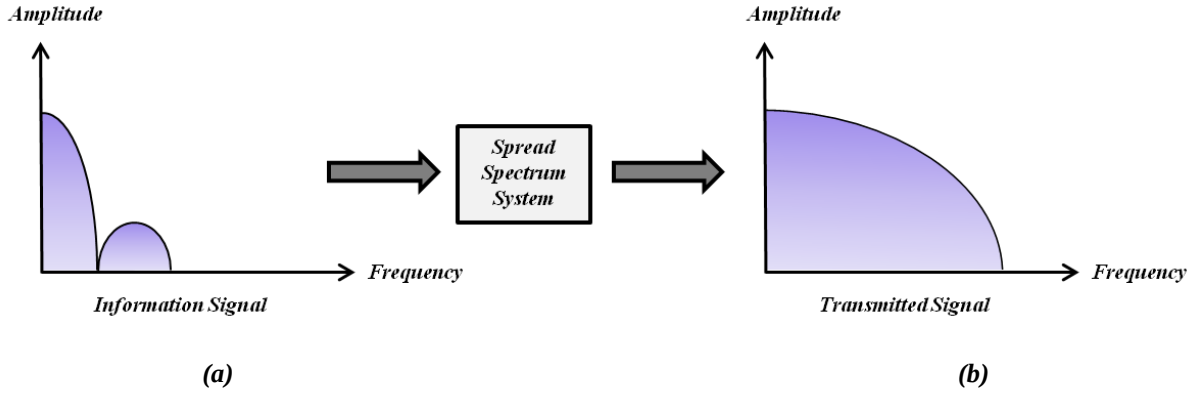

Figure 2.1: a) Bandwidth required to represent the information signal; b) Bandwidth utilized by the spread spectrum system for the transmission.

For instance, in OOK the data bit "1" is represented by the presence of optical pulse, and the data bit "0" is represented by the absence of optical pulse. OOK will be the modulation technique utilized in this work due to both its employment simplicity and intensity-modulation direct-detection (IM-DD) nature.

In OCDMA systems, each user's data bit is divided into time slots denoted as chips. A specific sequence of these chips forms a code sequence and to each user a distinct and unique code sequence is assigned. The total number of chips in each code sequence is determined by the code length. Moreover, the total number of short pulses (number of ones in each code) in each code sequence is determined by the code weight. The users use their own unique code sequences every time to transmit a data bit "1", represented by the presence of short optical pulses, whereas nothing is transmitted (absence of short optical pulses) for data bit "0". At the receiver side, the broadcasted signals are correlated with an already known code sequence in order to get the desired signal correctly decoded.

Normally, the set of codes employed in OCDMA systems should satisfy some correlation properties like, for instance, out-of-phase autocorrelation and cross-correlation properties in order to support a large number of simultaneous users in the system. Typically, the code set construction algorithm seeks to both maximize the autocorrelation in order to obtain the maximum orthogonality (degree of differentiation between codes) as well as to minimize the cross-correlation among the codes in order to obtain the maximum cardinality (number of available codes). Since the number of available codes provides the possible total number of users in a system, then the higher the code cardinality, the higher the number of users that can be accommodated in a system.

In this context, codes employed in OCDMA systems can be classified into time domain, frequency domain, spatial, phase or a combination of these. When only one of these dimensions is adopted, these codes are classified as one-dimensional (1-D). In the same way, when two or three dimensions are taken into account then one has two-dimensional (2-D) and three-dimensional (3-D) codes, respectively. Due to the high implementation complexity of 3-D codes, they will not be subject of study in this work. Next, the basic characteristics of 1-D and 2-D codes often found in OCDMA system applications are described. This chapter ends with a detailed explanation about how errors occur in OCDMA systems.

2.1 1-D CODING

Code generation is certainly at the heart of the OCDMA technology. A good choice of coding schemes impacts positively not only the orthogonality and cardinality of the generated code sequences, but also the overall system performance. Currently, there are many coding schemes available to perform the encoding and decoding of users' data in OCDMA systems. The first technique proposed for this task is known as temporal coding, which encodes a bit of information dividing it into small chips which are then spread in time within the original bit period. An alternative coding scheme consists in en-/decoding the users' data bit using only the spectral domain, a technique known as frequency coding. Both techniques are also known as one-dimensional (1-D) coding.

Both of these coding schemes are based on incoherent optical sources, and employ unipolar pseudo-orthogonal family codes like for instance, *m*-sequence, Hadamard, and optical orthogonal codes (OOCs). OOCs with cross-correlation and out-of-phase autocorrelation less than or equal to one minimize the MAI in incoherent systems, though impose restrictions on the number of available code sequences for a given code length. In addition, OOCs are usually a very sparse code family having large length and small weight.

The quantity of available OOC sequences is limited by the well-known *Johnson bound*, which determines the total number of available codes [21]. Since this number of available codes is a function of the code parameters such as the cross-correlation, OOCs with good cross-correlation properties generally present low number of available codes, which means that 1-D codes may have low cardinality. The following two sub-sections describe in details 1-D coding schemes employed in time and frequency domains, respectively.

2.1.1 CODING IN TIME DOMAIN, DS-OCDMA

In a conventional system transmission, a bit corresponds to a pulse of duration T_b. When going through the process of coding, this bit period will be divided into L subintervals of duration T_c denominated as chips. Figure 2.2 illustrates this concept for the case of a four bits sequence {1 0 1 1}, uncoded (top) and coded (bottom). Since the coding process applies the code sequence directly to the user data bit entering the modulator, this technique is defined as direct-sequence (DS) spread spectrum, which results in a DS-OCDMA system. The schematic diagram of an all-optical encoder and decoder for incoherent 1-D DS OCDMA is shown in Figure 2.3. As in the first coding implementations, the time allocation of pulses is achieved by means of optical delay lines (ODLs) as shown in Figure 2.3(a). This scheme allows for the generation of unipolar 1-D OOC family of codes. The matched filter at the decoder side is obtained by means of inverted delay lines with respect to those in the encoder.

The encoder consists of a $1 \times W$ splitter, with W delay lines plus a $W \times 1$ combiner. As shown in Figure 2.3(a) the number of delay lines is equal to the code weight, and the delay of each line is equal to the nonzero position of the code. In this scheme, the user's information bit is converted into a sequence of W chips with both high amplitude and short duration, where the duration of each chip, T_c, is related to the weight adopted by the code. Thus, $T_c = T_b / L$, where L is the code length that represents the number of chips in which T_b is fragmented. Similarly, the decoder, Figure 2.3(c), consists of a $1 \times W$ splitter, with W delay lines plus a $W \times 1$ combiner. Note that the delay of the corresponding lines at the encoder, Figure 2.3(a), and decoder, Figure 2.3(c), are complementary to each other.

In the encoding process, a sequence of short pulses proportional to the code weight, W, is formed. The code weight defines the number of illuminated chips as shown in Figure 2.3(b) for $W = 4$. During the decoding process, a set of similar ODLs with inverted configuration relative to that used in the encoder is used at the receiver to reconstruct the original pulse, Figure 2.3(c). In this case, the decoding operation is carried out by correlation intensity, in which pulses positioned correctly form a pattern defined by the autocorrelation property, otherwise they form a background interfering signal defined by the cross-correlation property, see Figure 2.3(d). Errors will occur in the decoder whenever the desired user transmits a bit “0”, and all the nonzero positions of the desired code are filled up with chips of interfering users. Further details about this issue are given at the end of this chapter.

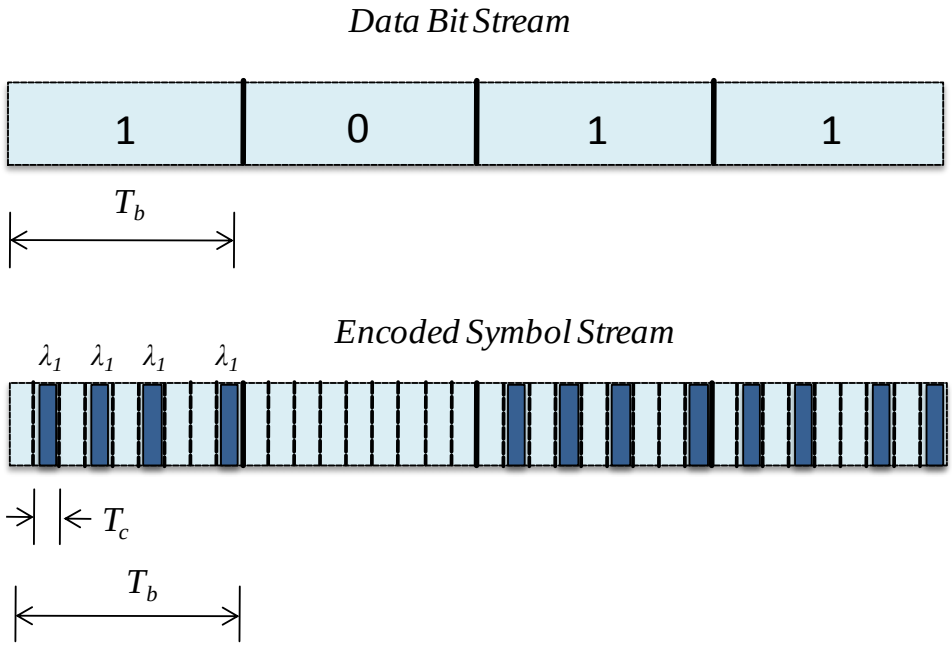

Figure 2.2: Bit stream through temporal coding scheme based on direct-sequence technique, DS-OCDMA.

In addition to traditional ODLs [64], other techniques have been suggested such as the use of photonic crystals [65] and integrated optics [66].

One of the first code schemes for incoherent DS-OCDMA systems was proposed by Salehi et al. [30], which consisted of an OOC with fixed equal length and weight for the entire code set. This ensures both the same transmission rate and BER for all system's users. Normally, OOCs are generated using passive components such as optical delay lines, optical splitters, and optical combiners as illustrated in Figure 2.3.

Recently, OOC with arbitrary code weights and different code lengths was proposed aiming at multiple rates and multiple-QoS (or equivalently, multiple-BER) transmission [58]. This OOC is referred to as multi-weight, multi-length OOC (MWML-OOC) [58]. The supported services and rates are directly related to the weight and length of the codes respectively, i.e., the different code weights provide service differentiation (multi-QoS), while the different code lengths provide data rate differentiation. Thus, the high-weight and short-length codes are assigned to high-QoS and high data rate users, respectively.

Usually, a MWML-OOC set is defined by the quadruple $(L, W, \lambda_a, \lambda_c)$ with unipolar (0, 1) sequences, where L, W, λ_a, and λ_c are the code length, code weight, maximum nonzero shift autocorrelation, and maximum cross correlation, respectively. In addition, a MWML-OOC code set with out-of-phase autocorrelation and cross-correlation bounded by maximum

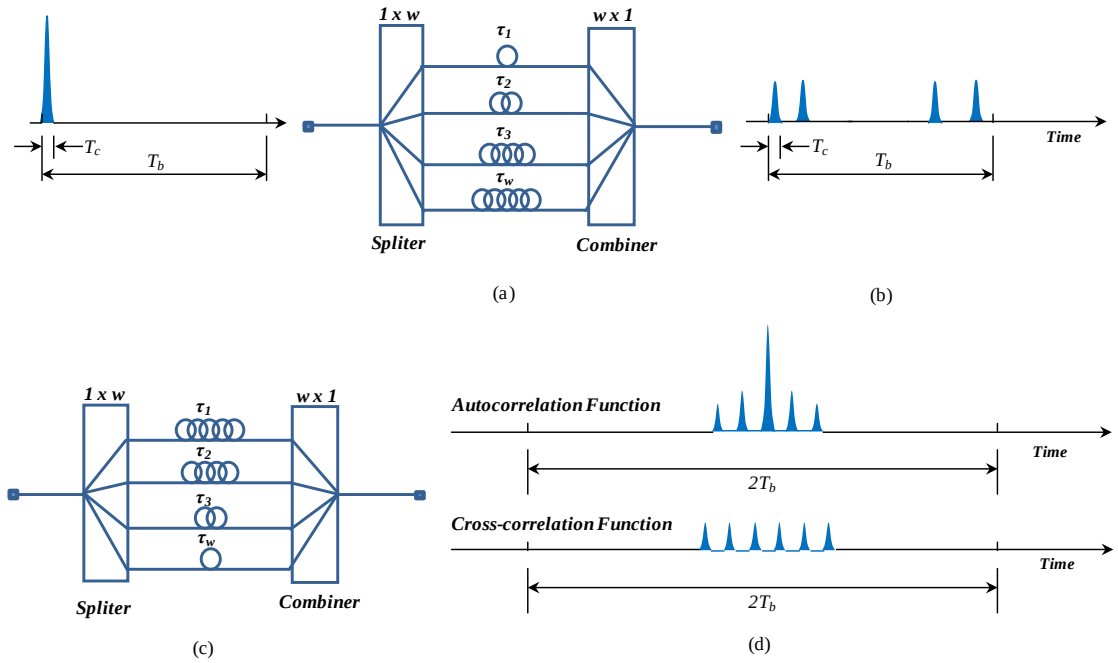

Figure 2.3: Coding in time domain using optical delay lines (ODLs): a) 1-D Encoder; b) Encoded signal; c) 1-D Decoder; d) Autocorrelation function; e) Cross-correlation function.

one, i.e., $\lambda_a = \lambda_c = 1$ are classified as strict codes, and can be represented in short as *(L, W, 1)*. It is worth mentioning that all code families employed in this work are classified as strict codes.

In order to proceed to the simulation of the OCDMA system, it becomes necessary to describe the en-/decoding process in mathematical terms. To do so, it is assumed that each bit is encoded in a waveform *s(t)* which corresponds to its code signature sequence. Each receiver correlates its code mask, *f(t),* with the transmitted signal *s(t)* [67]. Then, the output from the receiver *r(t)* is a correlation operation which shows the similarity degree between them, and is given by

$$r(t) = \int_{-\infty}^{\infty} s(\tau)\, f(\tau - t) d\tau. \qquad (1)$$

Normally, the codes' construction algorithms seeks to maximize the autocorrelation, *s(t) = f(t)*, and to minimize the cross-correlation between codes, *s(t) ≠ f(t)*, in order to obtain the maximum orthogonality i.e., degree of differentiation between them, and also cardinality i.e., number of available codes. The general conditions for the orthogonality of codes are [29]

1) Each code version can be distinguished from a shifted version of itself;
2) Each code version (possibly a shifted version) can be distinguished from each of all other sequences.

Hence, let's consider two sequences of length L, $X = \{x_0, x_1, ..., x_{L-1}\}$, and $Y = \{y_0, y_1, ..., y_{L-1}\}$ respectively. There are, then, the following correlation results that represent the interactions between them [30]:

i) For sequence $X=x(k)$:

$$|Z_{x,x}| = \left| \sum_{i=0}^{N-1} x_i x_{i+k} \right| = \begin{cases} W, & for \quad k=0 \\ \leq \lambda_a, & for \quad 1 \leq k \leq L-1 \end{cases} \tag{2}$$

ii) For each sequence pair $X=x(k)$ and $Y=y(k)$:

$$|Z_{x,y}| = \left| \sum_{i=0}^{N-1} x_i y_{i+k} \right| \leq \lambda_c, \quad for \quad 1 \leq k \leq L-1 \tag{3}$$

Where $Z_{x,x}$ and $Z_{x,y}$ corresponds to the autocorrelation of X and cross-correlation of X and Y, respectively. L is the code length, W is the code weight, λ_a is the out-of-phase autocorrelation peak, i.e., side lobes that correspond to shifted versions of a same sequence $k \neq 0$, and λ_c represents the cross-correlation peak between different sequences. Ideal orthogonality would be achieved when $\lambda_a = \lambda_c = 0$. However, this is not possible since the manipulation of optical pulses occurs in signal intensity. Hence, it is crucial to choose coding schemes that minimize λ_a and λ_c.

2.1.2 CODING IN FREQUENCY DOMAIN, FE-OCDMA

In the spectral domain it is possible to manipulate either signals of coherent optical sources for the treatment of the phase, or to manipulate signals of incoherent optical sources for the treatment of the amplitude. OCDMA systems whose coding scheme is spectrally-

based are normally referred to as frequency encoded OCDMA (FE-OCDMA) systems. The main motivation for using this system is that the bandwidth of the signal is independent of the source bandwidth, which may be for instance an incoherent light-emitting diode (LED). Thus, the parameters that define the code are independent of the information to be transmitted.

The 1-D coding process is schematically illustrated in Figure 2.4 [68], [69]. Each transmitter uses a spectral amplitude mask as encoder in order to transmit or block certain frequency components. The receiver in turn is formed by a spectral amplitude mask identical to that used in the transmitter, also known as direct filter *A(w)*, plus a complementary mask known as complementary filter $\overline{A}(w)$, and by two balanced photodetectors.

During the decoding process, the outputs from the complementary filters are detected by two identical photodetectors connected in balanced mode. For an unmatched transmitter, half of the transmitted spectral components will be related to the direct filter, and the other half to the complementary filter. Since the balanced receiver output represents the difference between the outputs of the two photodetectors, then any mismatched signals is canceled out, while a matched signal is demodulated. The recovered signal is delivered in amplitude modulated (ASK) and a threshold device responsible for the bit decision is adopted. The spectral efficiency of FE-OCDMA systems deploying incoherent sources has been analyzed in [70].

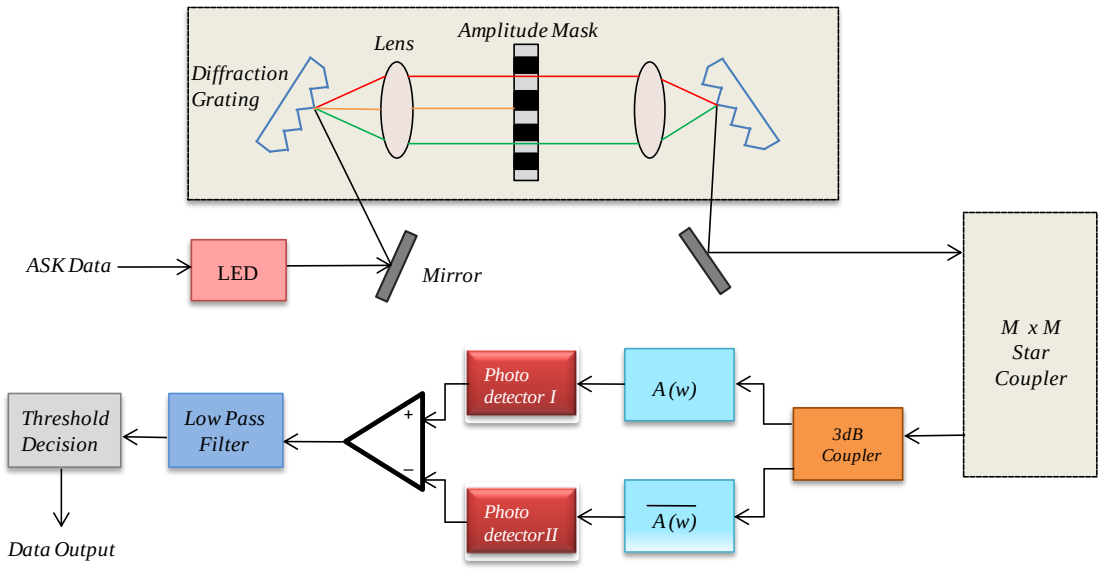

Figure 2.4: 1-D incoherent coding scheme based on spectral intensity, FE-OCDMA.

2.2 2-D CODING IN TIME AND FREQUENCY DOMAINS

An important issue regarding the first coding implementations using unipolar pseudo-orthogonal sequences is related to the inefficient use of bandwidth. An alternative to circumvent this issue is to manipulate both time and frequency domains simultaneously by employing 2-D family codes. Two dimensional codes are of particular interest since they allow considerable reduction in the temporal dimension of code sequences in relation to 1-D codes without worsening code cardinality or system performance, and further they satisfy more easily the required code correlation properties [71]-[73].

Accordingly, it has been proposed to add the wavelength dimension to the code design in order to construct codes with larger cardinality while maintaining good auto- and cross-correlation properties. In a 2-D coding technique, the chips' allocations are carried out simultaneously both in time and wavelength. In this case, the time and wavelength selections are decided according to a code construction algorithm, which not only increases the flexibility of the code design but also improves the cardinality dramatically.

Furthermore, in this type of coding scheme the code sequences are characterized by frequency hopping (FH). If a hop occurs in a time slot smaller than the information signal period the process is defined as fast frequency hopping (FFH), in which case fast jumps occur at wavelengths that change for every pulse of a given temporal sequence. The difference between FH and FFH signals in terms of frequency hopping occupancy is depicted in Figure 2.5. It can be observed from this figure that as time advances the signal occupies a separate frequency band as determined by the pseudo-random hopping code sequence. It can be further observed that hops in FFH must be to an exclusive frequency, i.e., to a frequency different from the previously utilized. Therefore, optical FFH (or OFFH) is a promising 2-D code to be implemented in multirate OCDMA systems. Both frequency hopping techniques are described in more details in the next sub-sections.

Generally, a 2-D frequency-hopping pattern can be represented in a $m \times n$ matrix form, with the number of lines, m, associated with the available wavelengths, and the number of columns, n, associated with the chip interval i.e., the temporal code length. Assuming orthogonality for the different wavelengths (neglecting interactions), implies that the shiftings are performed only in time. The correlation functions for a discrete 2-D system are defined as [72]:

i) For out-of-phase autocorrelation of x:

$$Z_{x,x} = \sum_{i=0}^{m-1} \left(\sum_{j=0}^{n-1} x_{i,j} x_{i,(j+\tau) \bmod (n)} \right) \leq \lambda_a \qquad (4)$$

ii) For cross-correlation between x and y:

$$Z_{x,y} = \sum_{i=0}^{m-1} \left(\sum_{j=0}^{n-1} x_{i,j} y_{i,(j+\tau) \bmod (n)} \right) \leq \lambda_c \qquad (5)$$

for any integer τ defined in the interval $0 < \tau < n$, where τ is the time delay. $Z_{x,x}$ and $Z_{x,y}$ correspond to the autocorrelation and cross-correlation functions, respectively. λ_a is the autocorrelation out-of-phase peak that corresponds to the side lobes ($\tau \neq 0$), and λ_c is the cross-correlation peak. The autocorrelation in phase is equal to the weight $Z_{x,x}\ (\tau = 0) = W$.

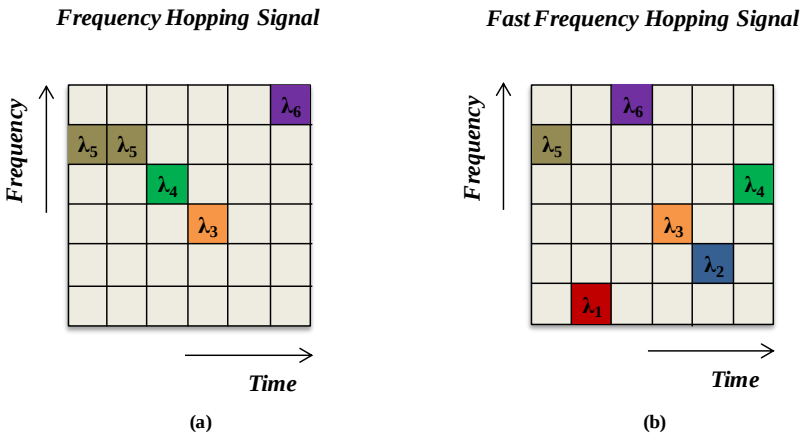

Figure 2.5: Frequency hopping technique. a) Time and frequency occupancy of frequency-hopping (FH) signal; b) Time and frequency occupancy of fast frequency-hopping (FFH) signal.

2.2.1 FREQUENCY HOPPING, FH-OCDMA

In frequency hopping, the carrier frequency of the transmitter hops in accordance with an apparently random pattern. This pattern is in fact a pseudo-random code sequence. The order of the frequencies selected by the transmitter is taken from a predetermined set as dictated by the code sequence. 2-D wavelength-hopping time-spreading (WH/TS) was proposed [71], [72], [74] as an alternative to overcome the shortcomings of 1-D codes.

A 2-D WH/TS is a family of codes based on 2-D FH coding capable of performing frequency spreading in time and wavelength domain simultaneously. It is worth mentioning that this code family covers many coding schemes proposed in the literature like, for instance, prime code/optical orthogonal code (PC/OOC) [21], [75], multiple-wavelength optical orthogonal code (MWOOC) [76], and one-coincidence frequency-hopping code/optical orthogonal code (OCFHC/OOC) [73]. The OCFHC/OOC should receive special attention due to its good performance [38], [50], and good code generation characteristics since the code length can be chosen independently of the number of available wavelengths without sacrificing good correlation properties.

Frequency hopping codes provide a significant increase in code cardinality, allowing for a larger number of active users in the system. In addition, it provides greater flexibility on the choice of code parameters. Figure 2.6 illustrates an example of 2-D WH/TS code sequence.

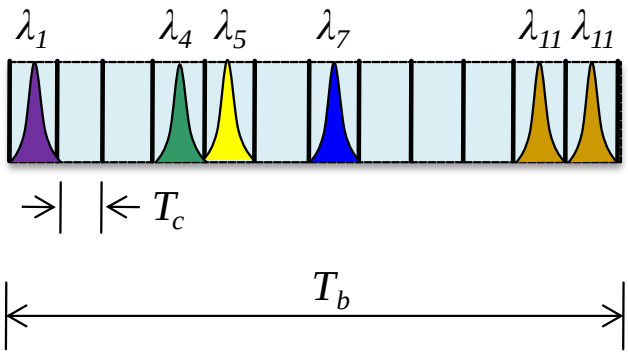

Figure 2.6: Example of a WH/TS code sequence.

It can be observed from this figure that some chip positions are not filled up and that the same wavelength has been used twice (this never happens in FFH).

Figure 2.7 illustrates a 2-D optical encoder/decoder suitable for WH/TS OCDMA [21]. The encoder in Figure 2.7(a) consists of a $1 \times W$ wavelength-division demultiplexer, W delay lines, and an $W \times 1$ wavelength-division multiplexer. Firstly, in the coding process, a short pulse corresponding to data bit "1" is separated by the wavelength-division demultiplexer into W pulses using a pre-established wavelength set. Next, the W pulses are delayed by their respective ODLs. Lastly, the pulses are combined and output by the wavelength-division multiplexer. Similarly, the decoder in Figure 2.7(b) consists of a $1 \times W$ splitter, with W delay lines, and an $W \times 1$ wavelength-division multiplexer. Note that the time delays produced by the corresponding delay lines at the encoder and decoder are complementary to each other. When the decoder outputs an autocorrelation peak, the data bit are correctly restored after optical-to-electrical conversion and threshold decision. The performance of a 2-D WH/TS OCDMA system has been investigated in [38], [50].

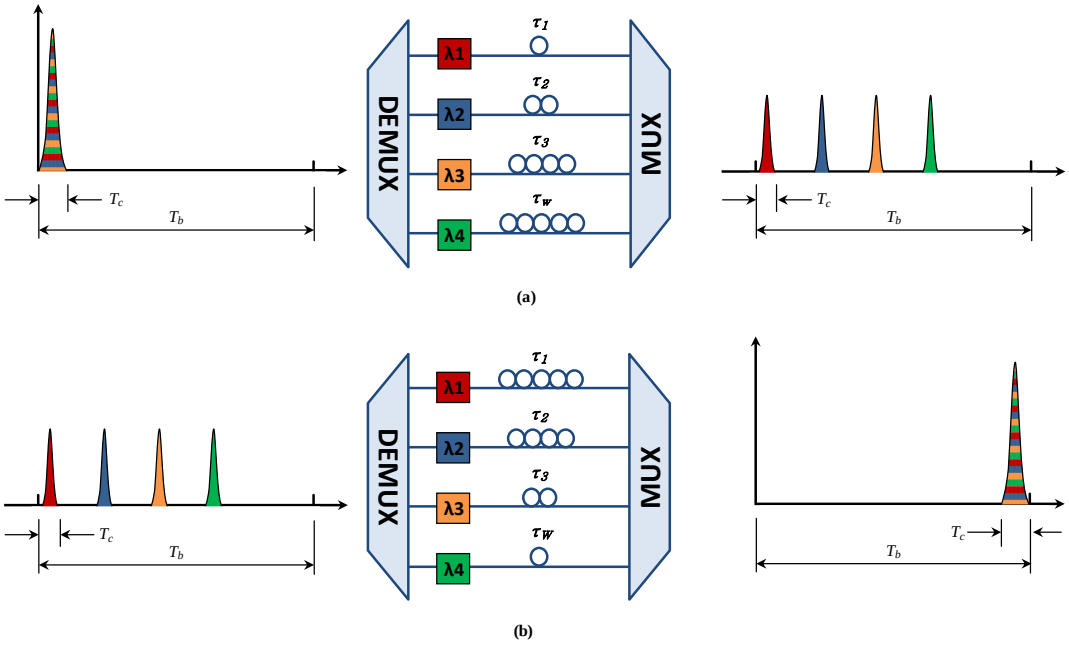

Figure 2.7: 2-D incoherent coding scheme based on time and frequency spreading, WH/TS OCDMA. a) Encoder using ODLs, multiplexer (MUX) and demultiplexer (DEMUX); b) Decoder using ODLs, MUX, and DEMUX.

2.2.2 FAST FREQUENCY HOPPING, FFH-OCDMA

The OFFH-CDMA system was originally proposed by Fathallah [45], and is based on a series of multiple Bragg gratings (MBGs) [77] in order to generate fast hopping frequency patterns. These gratings spectrally and temporally slice an incoming broadband pulse into several components generating then optical frequencies patterns, as can be seen in Figure 2.8. The passive all-optical signal coding based on MBGs allows both low-cost and robust implementation of OFFH-CDMA systems [78]. In this text, FFH-OCDMA and OFFH-CDMA are used interchangeably.

An inherent characteristic of OFFH systems is that the frequency changes at a significantly higher rate than the information rate, which means that each pulse in a code sequence is transmitted at an exclusive wavelength. Thus, OFFH systems are defined by several frequency hops within each data bit.

The first OFFH-CDMA system approach capable of achieving multiple rates was proposed by Inaty et al. [61], [53]. This system achieves multiple rates through different code lengths while keeping constant the chip period. This eventually entails in encoders and decoders pairs of different lengths, i.e., different quantity of Bragg gratings. A possible multirate architecture for OFFH-CDMA systems depicting both low rate user encoder (12 gratings) and high rate user (6 gratings) encoder is illustrated in Figure 2.8. This figure shows two FBGs structures with gratings deployed in series designed in this example to reflect the following 12 wavelengths λ_3, λ_5, λ_1, λ_{10}, λ_8, λ_4, λ_{11}, λ_6, λ_{12}, λ_9, λ_2, *and* λ_7 for low rate user, Figure 2.8(c), and the following 6 wavelengths λ_{25}, λ_{13}, λ_{28}, λ_{18}, λ_{15}, *and* λ_{20} for the high rate user, Figure 2.8(d), respectively. It is important to observe that any of the frequencies can be used more than once into the same code sequence [78].

The time-frequency hopping patterns that compose the transmitted signals are formed by the wavelength subset matrices presented in Figures 2.8(e) and 2.8(f) for low and high rate users, respectively. Since the broadband signal is determined to work as on-off keying (OOK), when the data bit value is “1”, an optical broadband short pulse is transmitted to the MBGs, otherwise no power is transmitted to the MBGs. Following this reasoning, the encoding technique will generate independent frequency pulses and places each of them in an appropriate time-frequency place as previously established by the OFFH hopping sequence pattern [78].

It is worth mentioning that this coding scheme is based on a convolution of an incoherent short pulse modulated by the data source with the response of each Bragg grating. This type of encoder can be considered a logical combination of the first two 1-D encoders previously described in Sections 2.1.1 and 2.1.2 of this chapter. As can be observed in Figure 2.8, while the Bragg gratings produce the frequency spectrum slicing, the Bragg gratings' position produce the respective time delays in a similar fashion to the ODLs in 1-D coding. The response of each Bragg grating is defined as the inverse Fourier transform of the grating complex reflectivity, where the incident pulses associated with the transmitted data are normally much narrower than the response duration of the grating.

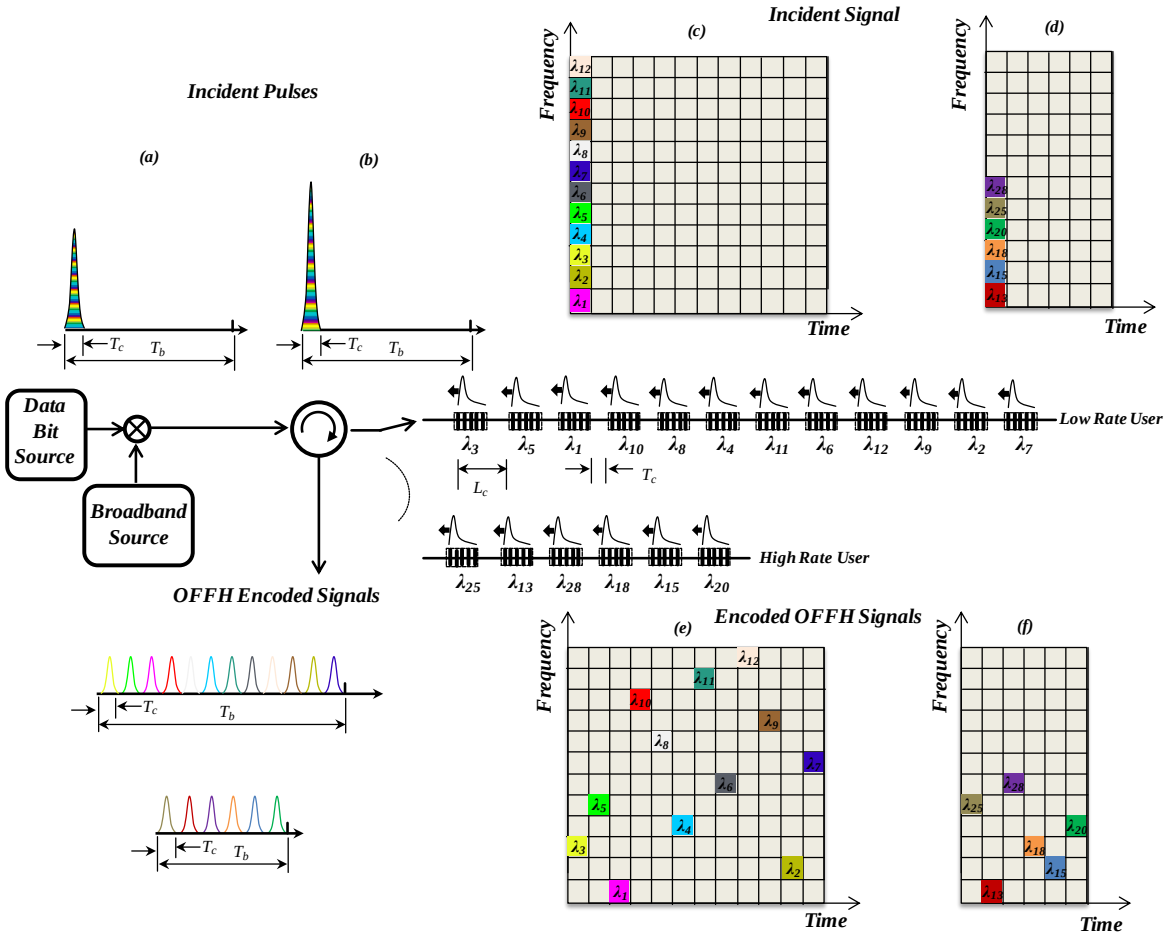

Figure 2.8: 2-D incoherent OFFH-CDMA transmitter implementation scheme employing MBG. (a) High rate user's incident broadband signal; (b) Low rate user's incident broadband signal; (c) and (d) Time-frequency hopping patterns matrix representation of the low and high rate users respectively before encoding; (e) and (f) OFFH hopping patterns matrix representation of the low and high rate users respectively after encoding.

In addition, the time frequency hopping pattern is determined by the order of the grating frequencies in the fiber since the multiple Bragg grating follow a first-in, first-reflected concept [45]. The chip duration, and the number of gratings in the encoder establishes the nominal data bit rate of the system, i.e., all reflected pulses of a data bit should leave the encoder before the next bit's pulses come in [79].

At the decoder, the wavelengths are placed in the reversed order of that placed in the encoder in order to accomplish the decoding function. This scheme is illustrated in Figure 2.9. Finally, the matched filter based-decoder removes the translation between the wavelengths and realigns all chips from the received signal, Figures 2.9(a)-(b), into a single pulse as shown in Figures 2.9(c)-(d), respectively.

As can be seen in Figure 2.9(e), pulses positioned correctly form a pattern defined by the autocorrelation property (similarity level between the transmitted and received desired signal), otherwise it will form a background interfering signal defined by the cross-correlation property known as MAI. The decoding operation in the receiver is, in turn, a sum of powers. Thus implies the quadratic detection law, where an electric current is generated directly proportional to the incident optical intensity. Hence, the phase spectrum of the grating does not need to be coherently added.

In OFFH coding, the available bandwidth is subdivided into contiguous frequency intervals, where the transmitted signal occupies a frequency range in each chip interval $T_c = \{[2 \times n_{eff} \times L_s] / c\}$, where L_s is the sum of one grating length plus one spacing distance between an adjacent grating, n_{eff} is the effective index, and c is the light speed [53]. Since the Bragg gratings are equally spaced, i.e., T_c is constant, the pulses are correspondingly spaced at time intervals T_c seconds apart from each other, which corresponds to the round-trip time (RTT) between two consecutive gratings [45]. The bandwidth associated with the data rate is $B = 1 / T_b$, and $T_b = \{[2 \times (L - 1) \times n_{eff} \times L_s] / c\}$, where L is the code length (also equivalent to the number of gratings) [53]. The gratings are written at the wavelength λ_B (Bragg wavelength) and tuned to different wavelengths ($\lambda_1, \lambda_2, ..., \lambda_F$) which are allocated in time intervals in accordance to the adopted algorithm. The parameter F accounts for the total number of available wavelengths. The Bragg wavelength of each grating ($\lambda_1, \lambda_2, ..., \lambda_F$) should thus comply the code needs, and be allocated in time intervals according to the adopted algorithm.

Concurrent support of multiple data rate transmissions can be achieved simply by changing the bit period, either by increasing or decreasing it whenever lower or higher bit

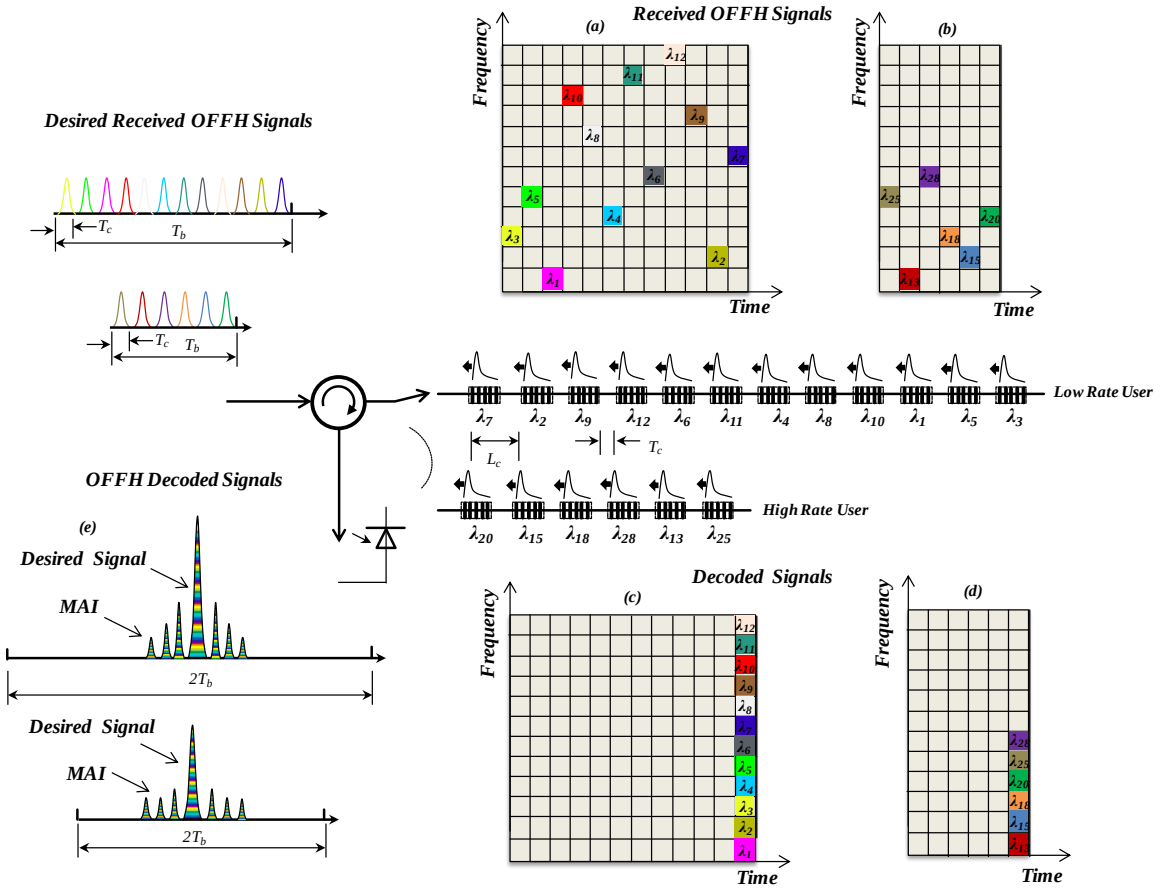

Figure 2.9: 2-D incoherent OFFH-CDMA receiver implementation scheme employing MBG. (a) and (b) Low and high rate user matrix representation respectively of the received OFFH signal; (c) and (d) Low and high rate user matrix representation respectively of the decoded signal; (e) Desired (high peak) and interfering (sidelobes) decoded signals.

rates are required. In turn, changing the bit period is absolutely analogous to changing the total RTT since both represent the period necessary for all pulses to be reflected by the MBGs. Consecutively, a possible way to modify the bit period is to change the number of gratings. Note that changing the number of gratings is also equivalent to changing the code length as they are directly associated.

It is worth emphasizing that decreasing the duration of the total RTT that the signal takes to enter and exit the series of Bragg gratings causes a decrease in the code duration and, consequently, an increase in the transmission rate. Therefore, from the previous discussion, a traditional way to achieve multirate transmissions in OFFH systems would be by changing the code length while keeping a fixed chip rate, which will eventually change the bit period.

Fiber Bragg gratings also offer the possibility of tuning the Bragg wavelength, which is very attractive for reconfiguring the encoder/decoder [78]. Accordingly, wavelengths from

longer code sequences can be tuned out the working bandwidth of the OFFH system therefore producing codes of different lengths and, consequently, allowing for multirate transmission. Actually, each Bragg grating can be individually tuned using piezoelectric devices in order to adjust an intended wavelength from an available wavelength range [78]. The wavelengths tuned out the working bandwidth are no longer reflected by the Bragg gratings of the encoder/decoder [53], i.e., the grating becomes transparent to these wavelengths. The tuning set of each pair of encoder-decoder will determine the code sequence employed. It can be clearly seen in Figure 2.8 that the frequency-hopping pattern of a high rate user is half the size of a low rate user once that some frequencies are not reflected any more. Note, though, that the frequency-hopping pattern does not necessarily have to be half the size as in this example. Furthermore, each of these grating contributes to a single reflected pulse. The number of available frequencies is limited by the tunability of the gratings, which establishes the system capacity. A possible manner to implement OFFH coding in practice is using the frequency-hopping patterns generated by the Bin's algorithm [80].

This algorithm employs $F \geq L$ for the code set construction. Further, the codes are classified as one-coincidence sequences [81], and are characterized by the following three properties: 1) all the sequences have the same length; 2) each frequency is used at most once in each sequence; 3) the maximum number of hits between any pair of sequences for any time shift equals one. These codes were originally proposed with equal lengths in order to achieve single rates. In spite of this, a possible manner to obtain OFFH-based codes with different lengths is to truncate longer code sequences in order to get shorter code sequences. Even though these codes have different lengths, they still preserve good correlation properties [82] as originally proposed. Figure 2.10 shows an example of two codes with different lengths that can be successfully employed to low rate and high rate users, respectively. It can be noted from this figure that although the bit period of the sequences is different, the chip period is the same and constant for both the sequences.

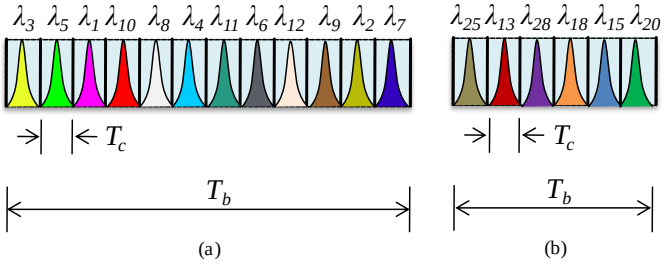

Figure 2.10: Example of multiple rate codes. (a) A large code sequence employed to low rate user; (b) A short code sequence employed to high rate user.

2.3 MULTIPLE-ACCESS INTERFERENCE (MAI)

In OCDMA systems, each user has a different signature sequence, i.e. an exclusive optical code characterizing the data of each user that will be transmitted simultaneously in the same channel. The different coding schemes currently available for 1-D codes [21], [22], [32], [46], [58] and for 2-D codes [21], [22], [38], [72], [75], [76] normally seek to achieve greater cardinality and orthogonality. Despite this, the use of codes that have good orthogonality do not ensure total differentiation between users' sequences, since the manipulation of optical pulses occurs by means of signal intensity [83].

For instance, let's consider a 2-D OCDMA system employing pulses shifted in time at various wavelengths, arranged according to a particular code generation algorithm. The information of each user is encoded with a specific sequence signature, multiplexed and sent to all receivers simultaneously. Each receiver has a replica of the signature code assigned to each user, which allows it to extract the received data information through the correlation operation. In the decoder side, the pulses at different wavelengths will overlap forming then an autocorrelation peak of high intensity for the case of the interest user. Otherwise, the pulses at different wavelengths will keep away from each other and cross-correlation signals with low intensity will be generated [51].

Furthermore, when the system accommodates many users simultaneously, the cross-correlation signals can accumulate and generate a power noise comparable to the autocorrelation peak [29]-[31]. This noise, denominated MAI, can cause a significant BER increase, and also severely limit the amount of users that can be accommodated on the system. Figure 2.11 illustrates how multiple simultaneous users contribute to the MAI for a particular user of reference. The user of reference is also known as the desired or target user, or even as user of interest. Note from this figure that the beginning of each user's sequence does not happen at the same time, showing clearly the asynchronous nature of users' access. It can be observed from the figure that the users have different code lengths and weights, which defines it as a multirate, multiservice (or differentiated services) interference scenario.

Consider the user of interest #1 whose code has illuminated chips at positions (2, 4, 6, 9). Detection errors normally occur when the user of interest is transmitting (receiving) a bit “0”. Note that user #2 interferes at the chip position 9 of user #1. Likewise, users #3, #4, and #5 will also interfere on user #1 at the positions 6, 4, and 2, respectively. The red vertical arrows indicate the chip positions on user #1 that will be affected by users #2, #3, #4 and #5,

respectively. This scenario illustrates how the MAI works, and how it may lead to detection errors.

Observe that MAI increases proportionally to the increase in the number of simultaneous users in the system, with a consequent degradation of the BER performance. Furthermore, observe that MAI does not cause errors during the transmission of data bit "1" by the desired user. This occurs because the interfering pulses always increase the channel energy, making it impossible for bit "1" to be detected as a bit "0". Therefore, when considering strict codes, i.e., codes with maximum cross-correlation and out-of-phase autocorrelation values bounded by one, errors will occur only when the desired user transmits a bit "0" and at least *W* (code weight) interfering users transmit bit "1" simultaneously on the system. This requirement of at least *W* users transmitting bit "1" simultaneously is due to the possibility of the unit cross-correlation codes (strict codes) contribute effectively at most with one pulse interference for the generation of errors.

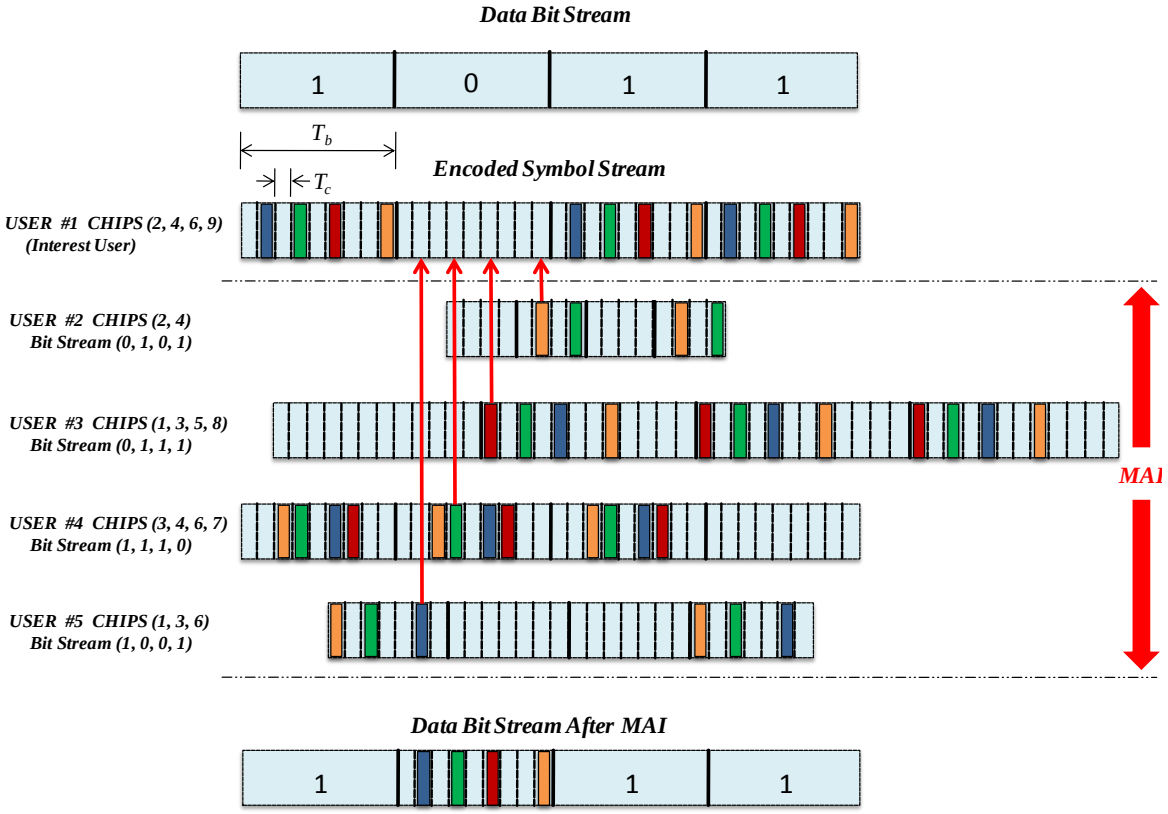

Figure 2.11: Example of the MAI contribution on the interest user #1 in an OCDMA network containing five simultaneous multirate users.

CHAPTER 3

NUMERICAL MODELING AND BER EVALUATION OF MULTIRATE OCDMA SYSTEMS

In this Chapter, it is presented the mathematical formalisms used to model the multirate, multiclass OCDMA system which includes new expressions for the evaluation of the BER in multirate, multiservice systems taking into account binomial and gaussian distributions for the MAI. For comparison's sake, the mathematical formalism assuming MAI as Poisson distributed [58] is also presented here.

The BER formalism proposed here for multirate OFFH-CDMA systems considering MAI as binomially distributed is original and represents an important contribution to the field. It should be emphasized that the proposed approach only requires the code parameters to be provided (not the users' code sequences), which makes the system analysis straightforward. In addition, the developed formalism can be applied to any multi-weight multi-length family of one- and two-dimensional codes with maximum cross-correlation and out-of-phase autocorrelation values bounded by one.

It is worth emphasizing that the main degrading factor of OCDMA systems is the MAI. MAI can be briefly defined as being the crosstalk among the many different users that share a common communication channel. MAI occurs when many users coexist simultaneously in the channel so that encoded unwanted users' signals generate noise, i.e., make interference on the code of the user of interest user. Furthermore, MAI is directly proportional to the number of simultaneous users in the system, so the higher the number of simultaneous users, the higher the level of MAI generated and, consequently, the higher is the signal degradation of the desired signal. This noise source severely limits the overall system performance.

The main focus of this work is to analyze OCDMA systems capable of providing multiple rates and multiservice transmissions, and for this purpose we will assume MAI as the only degrading factor of the system (ignoring fiber impairments and other sources of

noise). It is worth mentioning that the MAI probability distribution is not neither Poisson nor gaussian, and for many multirate, multiservice OCDMA scenarios these distributions might not be utilized as an accurate approximation, as will be shown later on Chapter 5.

The following sections describe in details how each MAI distribution is considered in the BER evaluation. Section 3.1 presents the new BER formalism for performance evaluation of multirate, multiservice OCDMA systems considering binomial distribution for the MAI. Section 3.2 is devoted to BER evaluation of multirate, multiservice MWML-OOC OCDMA systems considering Poisson distribution for the MAI. Finally, Section 3.3 presents the BER evaluation of multirate OFFH-CDMA systems considering gaussian distribution for the MAI.

3.1 BER EVALUATION CONSIDERING BINOMIAL DISTRIBUTION FOR MAI

Let's consider a multirate, multiclass OFFH-CDMA system capable of achieving multirate or multiservice (differentiated services) transmission through different code lengths by employing multiple fiber Bragg gratings in series [84]. The total number of users U in the J-class system is $U=\sum_{j=1}^{J} U_j$, where U_j is the number of users in class $j \in \{1,2,\dots,J\}$. The system employs OOK modulation, where power is transmitted for chip value equal to one, otherwise no power is transmitted.

For each class j of the J-class system, the users' rate is chosen by its corresponding code length given by $L_1 > L_2 > \cdots > L_j > \cdots > L_J$ in a way that high rate users have smaller code lengths and low rate users have larger code lengths, and $L_j = T_j / T_c$, where T_j is the bit period of class j users, and T_c is the chip period. These supported rates depend inversely on the code length, i.e., the shorter the code length, the higher the transmission rate.

Further, T_c is assumed constant and the same for all classes J, and the transmission power of all users U in all classes J is normalized to unity [58], [84]. Without any loss of generality, it is assumed that the desired user is the first user in the desired class denoted as j'. The transmitted intensity-modulated optical signal of the uth user in the jth class will be

$$S_{u,j}(t,f) = b_{u,j}(t)C_{u,j}(t,f), \tag{6}$$

where $b_{u,j}(t) \in \{0,1\}$ is the baseband signal of the *u*th user in the *j*th class, and $C_{u,j}(t,f) \in \{0,1\}$ is the uth user's hopping pattern of the *j*th class.

After going through the network, each user's signal will arrive to the receiver with the desired signal being degraded by MAI. Then, the received signal at the input of the decoder is given by

$$r(t,f) = \sum_{j=1}^{J} \sum_{u=1}^{U_j} S_{u,j}\left(t - \tau_{u,j}, f\right), \tag{7}$$

where $\tau_{u,j}$ is the time delay associated with the uth signal of the *j*th class. We consider only MAI on the detection of the desired user's bit $b_{1,j'}$. Hence, the decision variable at the matched filter output will be

$$Z = \int_0^{T_{j'}} r(t,f)\, C_{1,j'}(t,f)dt$$

$$Z = \sum_{u=1}^{U_j-1} I_{(j=j',u)}^{1,j'} + \sum_{j=j'+1}^{J} \sum_{u=1}^{U_j} I_{(j>j',u)}^{1,j'} + \sum_{j=1}^{j'-1} \sum_{u=1}^{U_j} I_{(j<j',u)}^{1,j'} + b_{1,j'} W_{j'}, \tag{8}$$

where $I_{(j=j',u)}^{1,j'}$, $I_{(j>j',u)}^{1,j'}$, and $I_{(j<j',u)}^{1,j'}$ are the interferences from the equal, longer, and shorter code length classes, respectively [84]. $W_{j'}$ is the user's code weight of class j'. The total MAI is then given by the sum of the interferences from all users' classes, denoted as $I_{j'}$ without any loss of generality. Therefore, (2) can be rewritten as

$$Z = I_{j'} + b_{1,j'} W_{j'}. \tag{9}$$

Next, it is derived the BER expression assuming that the MAI has a binomial distribution, since the output interference of any OCDMA system is considered to be binomially distributed [50], [55], [58], [84]. In addition, the MAI is assumed to be the main degrading factor of the system, as it is the most important noise source [45]. Moreover, it is assumed a chip synchronous scenario, which reflects the worse possible case for the system analysis [1], [50], [58].

Then, the moment-generating function of the binomially distributed total interference $I_{j'}$ becomes [58]

$$M_{I_{j'}}(t) = E\left[e^{tI_{j'}}\right] = \prod_{j=1}^{J} (1 - p_{jj'} + p_{jj'}e^{t})^{N_j}, \tag{10}$$

where N_j is the number of interfering users in class j, and $p_{jj'}$ is the total probability of interference caused by a code of class j on a code of class j' and is written as [84]

$$p_{jj'} = \frac{W_j W_{j'}}{2L_j F}, \tag{11}$$

where F is the total number of available wavelengths. For the case of a unique single-rate system, the probability of interference reduces to $p_{j'j'} = W^2/2LF$ [85], where $W = W_{j'}$ and $L = L_{j'}$. It should be mentioned that the user code of class j with W_j chips out of L_j chips have pulsed signal and can hit on any of the $W_{j'}$ chips of the class j' users [1], [84]. Recall that in OFFH the code weight W_j is equal to the code length L_j, thus $W_j = L_j$. Further, the parameter F accounts for the wavelength dimension of the code design created by the OFFH [85]. The term ½ in (11) results from the equal probability of each user transmitting on-off pulses with OOK modulation.

Next, the mean and variance of the MAI can be obtained as

$$\eta = M'_{I_{j'}}(0) = \sum_{j=1}^{J} N_j \, p_{jj'}, \tag{12}$$

and

$$\sigma^2 = M''_{I_{j'}}(0) - \left[M'_{I_{j'}}(0)\right]^2 = (U-1)\mathcal{P}(1-\mathcal{P}), \tag{13}$$

respectively. Since the mean of such MAI is also given by $\eta = \mathcal{P}(U-1)$, then we have [84]

$$\mathcal{P} = \sum_{j=1}^{J} \frac{N_j p_{jj'}}{(U-1)}, \tag{14}$$

where $\mathcal{P}$ is the multirate probability of interference. Thus, using the above definitions, the probabilities of error when a bit "0" and "1" are sent will be [84]

$$P(error|0) = \sum_{i=\mu}^{U-1} \binom{U-1}{i} \mathcal{P}^i (1-\mathcal{P})^{U-1-i}, \tag{15}$$

and

$$P(error|1) = \sum_{i=0}^{\mu-1-W_{j'}} \binom{U-1}{i} \mathcal{P}^i (1-\mathcal{P})^{U-1-i}, \tag{16}$$

where $P(error|0)$ and $P(error|1)$ are both the probability of false alarm and the probability of false dismissal, respectively [48], and μ is the threshold value of the decision device.

Considering MAI as the only degrading factor of the system, a general choice of μ, and also equiprobable data, it is obtained the BER of class j' users using both (15) and (16) as [84]

$$BER(j') = P\left(Z \geq \mu \middle| b_{1,j'} = 0\right) \cdot P\left(b_{1,j'} = 0\right) + P\left(Z < \mu \middle| b_{1,j'} = 1\right) \cdot P\left(b_{1,j'} = 1\right)$$

$$BER(j') = \frac{1}{2}\left[P\left(Z \geq \mu \middle| b_{1,j'} = 0\right) + P\left(Z < \mu \middle| b_{1,j'} = 1\right)\right]$$

$$BER(j') = \frac{1}{2}\left[\sum_{i=\mu}^{U-1} \binom{U-1}{i} \mathcal{P}^i (1-\mathcal{P})^{U-1-i} + \sum_{i=0}^{\mu-1-W_{j'}} \binom{U-1}{i} \mathcal{P}^i (1-\mathcal{P})^{U-1-i}\right] \tag{17}$$

It is worth pointing out that (17) is general and denotes not only the BER of an OFFH system, but also the BER of most multiclass, multirate systems providing that the corresponding code parameters ($W_j, W_{j'}, L_j, L_{j'}, and\ F$) are employed. For instance, to obtain the BER of a MWML-OOC OCDMA system [8], [58] one should employ its corresponding code parameters, and also make $F = 1$ in (11), due to the 1-D code in consideration [84].

3.2 BER EVALUATION CONSIDERING POISSON DISTRIBUTION FOR MAI

Consider a strict MWML-OOC OCDMA system capable of achieving multiple rates and multi-QoS through both different code lengths $L_1 \leq L_2 \leq \ldots \leq L_j \leq \ldots \leq L_J$ and arbitrary code weights W_j respectively [58]. The total number of users U in the adopted J-class system is $U = \sum_{j=1}^{J} U_j$, where U_j is the number of users in each class $j \in \{1, 2, \ldots, J\}$. Without any loss of generality, it is assumed that the desired user is the first user in the desired class denoted as j'. In addition, the chip period of all users' classes is the same and is given by $T_c = T_j / L_j$, where T_j is the class-j bit period. Moreover, it is considered a chip synchronous scenario, which reflects the worse possible case for the system analysis [8], [50], [84]. Furthermore, the transmission power of all users U in all classes J is normalized to unity, and the received power of all users is equal [58], [84]. Also, the system employs OOK modulation, where power is transmitted for chip value equals to one, otherwise no power is transmitted.

Next, it is considered the effect of MAI on the detection of data bit represented as $b_{1,j'}$. Adopting $I_{jj'}$ as the sum of interference from the jth users class on the j'th user class the correlator output is then given by [58]

$$Z = W_{j'} b_{1,j'} + \sum_{j=1}^{J} I_{jj'}$$

$$Z = W_{j'} b_{1,j'} + I_{j'}, \tag{18}$$

where $I_{j'}$ is the total MAI generated from all users classes on the desired user's class j', and $W_{j'}$ is the code weight of the desired user. Afterwards, the moment-generating function of random variable $I_{jj'}$, which is binomially distributed will be [58]

$$M_{I_{jj'}}(t) = E\left[e^{tI_{jj'}}\right] = \left(\left(1 - p_{jj'}\right) + p_{jj'} e^{t}\right)^{U_j}. \tag{19}$$

where $p_{jj'}$ denotes the total probability of interference (hit) caused by a mark position of a code from interfering class j on a mark position of the code from the desired class j' (desired user), and this is written as [58]

$$p_{jj'} = \frac{W_{j'} W_j}{2N_j}, \tag{20}$$

The term ½ is due to the equal probability for a user transmits data bit "0" or "1" with OOK modulation.

Next, considering the total interference generated from all users classes $I_{j'}$, (15) can be further extrapolated as [58]

$$M_{I_{j'}}(t) = \prod_{j=1}^{J} M_{I_{jj'}}(t), \tag{21}$$

then the mean of the MAI can be obtained as

$$\mathbf{E}\left[I_{j'}\right] = M'_{I_{j'}}(0) = \sum_{j=1}^{J} U_j p_{jj'}, \tag{22}$$

where $\boldsymbol{E}(\cdot)$ is the expectation operator. The expected value of the total interference $I_{j'}$ squared can be obtained as

$$\mathbf{E}\left[\left(I_{j'}\right)^2\right] = M'_{I_{j'}}(0)$$

$$\mathbf{E}\left[\left(I_{q'}\right)^2\right] = \left(\sum_{j=1}^{J} U_j p_{jj'}\right)^2 + \sum_{j=1}^{J} U_j p_{jj'}\left(1 - p_{jj'}\right). \tag{23}$$

Since the variance of the MAI is given by $\sigma^2_{I_{j'}} = \boldsymbol{E}(I^2_{j'}) - \boldsymbol{E}^2(I_{j'})$, then the variance can be written as [58]

$$\sigma^2_{I_{j'}} = \sum_{j=1}^{J} U_j p_{jj'}\left(1 - p_{jj'}\right). \tag{24}$$

The binomially distributed interference $I_{jj'}$ can be approximated by a Poisson

distribution for large U_j and small $p_{jj'}$. Thus, according to this fact, the interference $I_{jj'}$ has the following Poisson distribution expressed as [58]

$$P_{I_{jj'}}(I_{jj'} = n) \approx \frac{(U_j p_{jj'})^n}{n!} e^{-U_j p_{jj'}}. \tag{25}$$

As the sum of independent and identically distributed random variables is also Poisson distributed, (25) can be extrapolated to the total interference $I_{j'}$ as [58]

$$P_{I_{j'}}(I_{j'} = n) \approx \frac{\left(\sum_{j=1}^{J} U_j p_{jj'}\right)^n}{n!} e^{-\sum_{j=1}^{J} U_j p_{jj'}}$$

$$P_{I_{j'}}(I_{j'} = n) = \frac{T^n}{n!} e^{-R}. \tag{26}$$

Considering MAI as the only degrading factor of the system, μ the threshold of the decision device, and also equiprobable data, it is obtained the BER of class j' users as [58]

$$P(E) = \frac{1}{2}\left[P(Z \geq \mu | b_{1,j'} = 0) + P(Z < \mu | b_{1,j'} = 1)\right] \tag{27} .(a)$$

$$P(E) = \frac{1}{2} P(I_{j'} \geq \mu | b_{1,j'} = 0) \tag{27} .(b)$$

$$P(E) \approx \frac{1}{2}\left[1 - e^{-R} \sum_{n=0}^{\mu-1} \frac{T^n}{n!}\right]. \tag{27} .(c)$$

Since the (optimum) threshold value is equal to the desired user's code weight, and that the positive properties of the optical channel is taken into account, then no decision error will occur when a data bit "1" is transmitted. Therefore the second term in (27).(a), that represents errors when data bit "1" is sent, is equal to zero.

3.3 BER EVALUATION CONSIDERING GAUSSIAN DISTRIBUTION FOR MAI

Consider a multirate, multiclass OFFH-CDMA system capable of achieving multirate or multiservice (differentiated services) transmission through different code lengths by employing MBGs in series [53], [84]. Thus the encoding and decoding procedures are realized passively using a series of MBGs. A traditional approach to achieve multirate transmission is to vary the code length and keep fixed the chip period, which eventually leads to a variation in the bit period.

In OFFH-CDMA systems the available bandwidth is divided into a number L_j of contiguous frequency slots, where to each user is assigned a unique frequency-hopping pattern as its own sequence code [45]. For each user of class-j, the code is composed by L_j frequencies from a range of F available frequencies $S = \{f_1, f_2, \dots, f_F\}$, where $L_j \leq F$.

The OFFH-CDMA system achieves multiple rates through different code lengths $L_1 > L_2 > \cdots > L_j > \cdots > L_J$, in a way that high rate users have smaller code lengths and low rate users have larger code lengths. The total number of users in the J-class system is $U=\sum_{j=1}^{J} U_j$, where U_j is the number of users in class $j \in \{1,2,\dots,J\}$ [84]. Without any loss of generality, it is assumed here that the desired user is the first user in the desired class denoted as j'. Again, the system employs OOK modulation, where power is transmitted whenever the chip values are equal to one. The transmitted signal will occupy one frequency slot in each chip signaling interval $T_c = T_j/L_j$, where T_j is the bit period of class j. Further, T_c is assumed constant and the same for all classes J, and the transmission power of all users U in all classes J is normalized to unity [58], [84].

Next, the BER expression is derived assuming, firstly, that the MAI has a binomial distribution and, lastly, that a possible approximation to this expression is to consider a gaussian distribution for the MAI. As in the previous cases, here is also considered a chip synchronous scenario, which reflects the worse possible case for the system analysis [50], [84]. Hence, assuming MAI as the only degrading factor of the system, a general choice of μ, and equal likelihood to transmit data bit "0" or "1", the BER expression of class j' users using both (9) and (10) becomes [84]

$$BER(j') = P\left(Z \geq \mu \middle| b_{1,j'} = 0\right) \cdot P\left(b_{1,j'} = 0\right) + P\left(Z < \mu \middle| b_{1,j'} = 1\right) \cdot P\left(b_{1,j'} = 1\right)$$

$$BER(j') = \frac{1}{2}\left[P\left(Z \geq \mu \middle| b_{1,j'} = 0\right) + P\left(Z < \mu \middle| b_{1,j'} = 1\right)\right]$$

$$BER(j') = \frac{1}{2}\left[\sum_{i=\mu}^{U-1} \binom{U-1}{i} \mathcal{P}^i (1-\mathcal{P})^{U-1-i} + \sum_{i=0}^{\mu-1-W_{j'}} \binom{U-1}{i} \mathcal{P}^i (1-\mathcal{P})^{U-1-i}\right] \quad (28)$$

In order to minimize the BER, the threshold is set to the optimum threshold value $W_{j'}$. Further, taking into account the additive and positive properties of the optical channel, no decision error will occur when a data bit "1" is sent, i.e., $P(error|1) = 0$ as it is always decoded correctly [1] Therefore, (28) reduces to

$$BER(j') = P\left(Z \geq \mu \middle| b_{1,j'} = 0\right) \cdot P\left(b_{1,j'} = 0\right) + P\left(Z < \mu \middle| b_{1,j'} = 1\right) \cdot P\left(b_{1,j'} = 1\right)$$

$$BER(j') = \frac{1}{2}\left[P\left(Z \geq \mu \middle| b_{1,j'} = 0\right) + P\left(Z < \mu \middle| b_{1,j'} = 1\right)\right]$$

$$BER(j') = \frac{1}{2}\sum_{i=\mu}^{U-1} \binom{U-1}{i} \mathcal{P}^i (1-\mathcal{P})^{U-1-i} \quad (29)$$

Knowing that the binomially distributed MAI converges to a gaussian distribution when the number of users in the system is large enough [45], [48] a gaussian approximation of the BER expression (29) can be obtained as follows [84]

$$BER_{GA}(j') = \frac{1}{2}\left[P\left(Z \geq \mu \middle| b_{1,j'} = 0\right) + P\left(Z < \mu \middle| b_{1,j'} = 1\right)\right]$$

$$BER_{GA}(j') = \frac{1}{2}\, Q\left(\frac{\mu - \eta}{\sigma}\right), \quad (30)$$

where σ is the square root of the variance, and *Q(.)* is the well-known *Q*-function defined as [45]

$$Q(x) = \frac{1}{\sqrt{2\pi}} \int_{x}^{+\infty} e^{-u^2/2} du \tag{31}$$

It is important to mention that this approximation is only acceptable provided that the number of users is large enough [48], [55], [58], [84] and the probability of interference from an interfering user is close to 0.5 [55], [58], [86]. In Chapter 5, it is analyzed an OFFH multirate scenario where these two conditions are not completely satisfied, therefore resulting in a really poor approximation.

CHAPTER 4

MULTIRATE, MULTISERVICE HYBRID OCDM/WDM OPTICAL PACKET SWITCH

Over the last few years, many different routing technologies such as time-division multiplexing (TDM), wavelength-division multiplexing (WDM), and optical code-division multiplexing (OCDM) have been investigated in optical fiber communications. Among these technologies, OCDM constitutes a strong candidate for next generation optical networks, particularly due to features like asynchronous operation, simplified network control, easy addition of new users, capacity on demand, high compatibility with others multiplexing techniques, and possibility of implementing differentiated-QoS and multiple rates at the physical layer [87]-[90]. Nowadays, there has been an increasing demand for new multimedia applications as previously discussed in Chapter 1. Accordingly, these new multimedia applications will require differentiated-QoS and multiple rates transmission, which is becoming a challenge for future optical networks [1].

Furthermore, in OCDM scheme each transmission channel is encoded with an exclusive code, whereby only the intended receiver with the correct codeword can recover the information. At the receiver, the desired signal from all other signals of the channel is recognized and decoded based on a matched filter, followed by a thresholding device. Basically, this process happens in the same way as in OCDMA. Therefore, at the physical layer, OCDM transport networks assign optical codewords to transmission channels in the same fashion as OCDMA networks assign codewords to users.

Currently, many differentiated-QoS and multiple transmission rate solutions have been proposed for OCDMA networks [1]-[8], [84] in order to supply the new user's demand for more bandwidth and services. Even though recent OCDMA literature has witnessed a growing activity in multirate, multiservice transmission little attention has been paid to its transport counterpart (OCDM) in this matter.

Nevertheless, the OCDM scheme is very attractive to be used together with WDM resulting in hybrid OCDM/WDM networks [62]. Also, the bandwidth granularity of WDM transport networks is improved when implemented together with OCDM. In [91] it was also demonstrated that the spectrum efficiency of hybrid OCDM/WDM could be twice as much the one obtained with WDM.

Contrary to the ordinary one-dimension wavelength routing in WDM network, OCDM/WDM network has two dimensions (code and wavelength) for routing, thus it is denominated as code/wavelength routing network [62]. In this network, bandwidth of a single wavelength is shared among many codewords and assigned to different channels, where these codewords are considered as labels.

In [62], a bufferless single service, single rate OCDM/WDM OPS is investigated taking into account impairments due to both MAI and beat noise. Two analytical models were proposed to dimension the switch resources. The first model dimensions the number of optical codes supported on each wavelength, and provides packet loss probability (PLP) performance evaluation considering both MAI and beat noise. The second model dimensions the number of wavelength converters in order to achieve the minimum PLP due to output packet contentions. Accordingly, a PLP expression considering packet contentions is also provided. Moreover, this switch employs coherent OCDM techniques by adopting Gold codes, where the coding is based on optical amplitude with each chip in the code sequence having a phase 0 or π with binary-phase-shift-keying (BPSK) scheme.

In this Chapter, it is presented a novel architecture of a hybrid OCDMA/WDM OPS capable of supporting multiservice, multirate transmission [92]. The main idea is to employ incoherent MWML-OOC as signature sequence of an incoherent OCDM scheme to achieve differentiated services and multiple rates. The architecture of the proposed hybrid switch is presented and described. An analytical model to analyze the multiservice switch performance is proposed. In order to evaluate the PLP performance of the hybrid switch, a BER expression based on binomial distribution for the MAI is derived. The incoherent multiservice switch is extremely interesting from a practical point of view, since it does not require any new optical processing as it employs basically the same mature optical technology utilized in single service hybrid OCDM/WDM switches.

4.1 MULTIRATE, MULTISERVICE HYBRID OCDM/WDM NETWORK DESIGN

Generally, OCDM can be divided into two categories depending on the way in which a given user's codeword is applied to the optical signal [90]: incoherent, where a unipolar code is used with on-off keying modulation format, and coherent, where carrier phase shifted optical chips pulse sequence is adopted. In this work, it is employed incoherent MWML-OOC family as signature sequence of an OCDM scheme to provide multiservice, multirate transmission in a hybrid OCDM/WDM network. In addition, these supported services and rates are directly related to the weight and length of the codes, respectively. That is to say, the different codeword weights support service differentiation (multi-QoS), and the different codeword lengths support data rate differentiation. The shorter the codewords, the higher the rates, and the higher the codewords weights, the higher the QoS [58]. Notice that the supported rates depend inversely on the codeword length.

Next, let's assume a MWML-OOC-based OCDM system capable of achieving multirate and differentiated QoS transmission through both different codeword lengths $L_1 \leq L_2 \leq \cdots \leq L_j \leq \cdots \leq L_J$ and arbitrary codeword weights W_j, respectively [8], [92]. The total number of codewords (and consequently of users) F in the J-class system is $= \sum_{j=1}^{J} F_j$, where F_j is the number of codewords in class $j \in \{1,2, \ldots, J\}$. Without any loss of generality, it is assumed that the desired user's codeword is the first user's codeword in the desired class denoted as j'. Furthermore, the chip duration of all classes is assumed constant and the same, and given by $T_c = T_j/L_j$, where T_j is the bit period of class j, and L_j is the class j codeword length.

The architecture of the proposed OCDM/WDM optical packet switch is illustrated in Figure 4.1 [92]. As can be seen, it has N planes for both N input fibers (IF) and output fibers (OF). In a given input plane, the wavelengths M of an input fiber are separated by a wavelength demultiplexer (*DEMUX*), and for each demultiplexed wavelength λ_m the decoder arrays of the defined classes (*DA_Cj*) decode the codewords of the incoming signals. The decoders of the respective codewords in the *j*th class are implemented in each decoder array (*DA_Cj*) (at any given wavelength λ_m and output plane). As an example of possible 1-D encoder/decoder refer please to Chapter 2, Section 2.1.1.

The switching fabric SF_A forwards the decoded codewords to either the pool of R wavelength converters (WC_R) or to the switching fabrics SF_i $(i = 1, \dots, N)$ based on the decisions taken by the control unit. The encoders of the respective codewords in the *j*th class are implemented in each encoder array (*EA_Cj*) (at any given wavelength λ_m and output plane).

All outputs of the encoder arrays (EA_C_J) are aggregated by a wavelength multiplexer (*MUX*), and the aggregated codewords are forwarded to the output fiber.

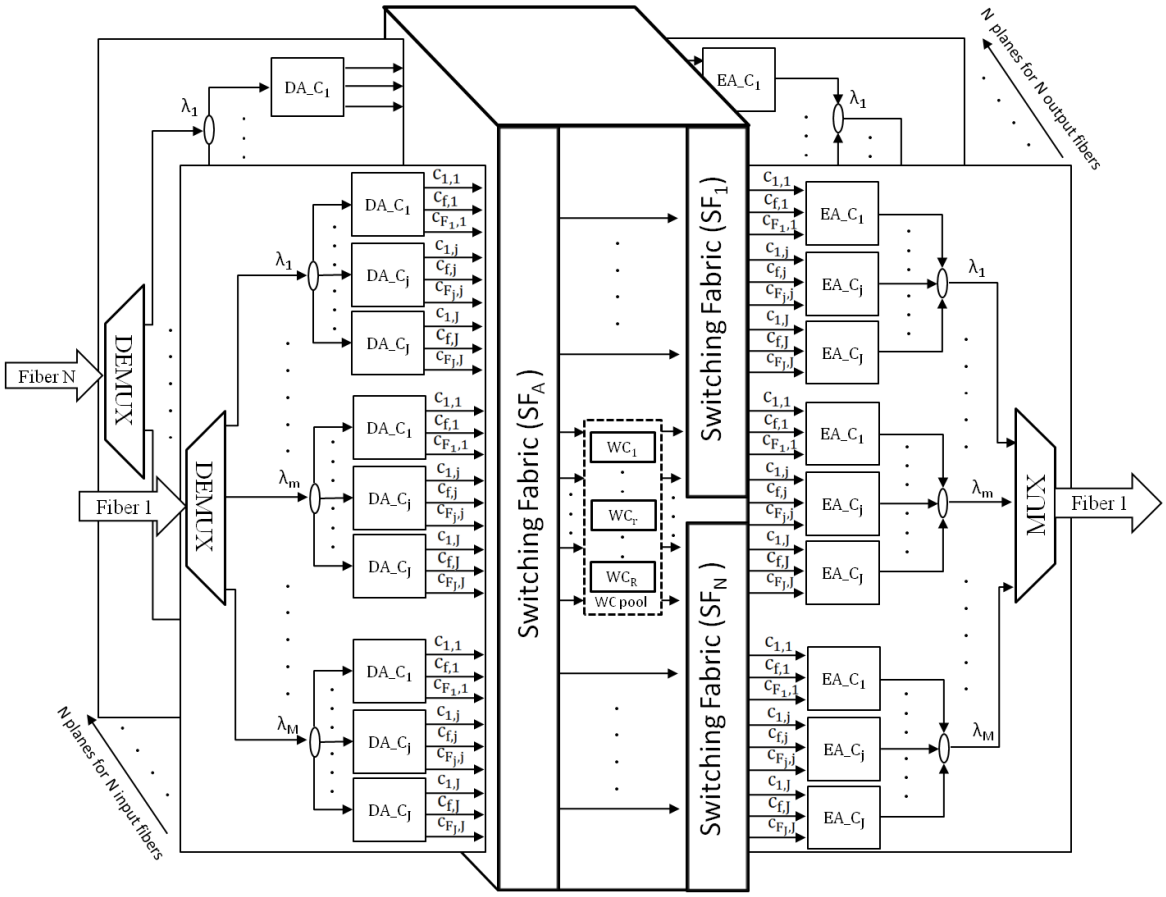

Figure 4.1: Multiservice OCDM/WDM optical packet switch.

Moreover, in this structure each input/output fiber supports *M* wavelengths denoted by $\lambda_1, \dots, \lambda_m, \dots, \lambda_M$. The total number of packets carried out on each wavelength by the OCDM scheme is *F*, and the number of packets in the *j*th class is F_j. It worth pointing out

that the number of users, codewords and packets are equal and are all accounted for by the same parameter *F*.

Further, the total code set of a wavelength on which packets can be carried out is given by $C = \{C_1, C_2, \dots, C_j, \dots, C_J\}$ where $C_j = \{c_{1,j}, c_{2,j}, \dots, c_{f,j}, \dots, c_{F_j,j}\}$ is the set of codes in class j, and $c_{f,j}$ is the *f*th code in the *j*th class. An input (or output) channel is identified by the triplet $(i, \lambda_m, c_{f,j})$, where *i (i = 1,…, N)* identifies one of the input (or output) fibers (IF or OF), and λ_m identifies one of the wavelengths in these fibers, and $c_{f,j}$ $(f = 1, \dots, F; j = 1, \dots, J)$ is used to identify an optical codeword in any class on that wavelength, respectively [92].

The multiservice OCDM/WDM packet switch shown in Figure 4.1 performs the following operations: (a) incoming packets on each input fiber are wavelength demultiplexed and decoded by means of one WDM demultiplexer and $M \times F$ codeword decoders; (b) the control unit processes the packet headers, handles packet contentions, and decides which packets have to be codeword and wavelength converted based on the rules of the scheduling algorithm [92]. Also, it decides which output wavelength channels and output codewords are assigned to the packets to transmit; (c) the switching fabric SFA routes the packets towards either the pool of R wavelength converters (WCR) or to the output switching fabrics SF_i $(i = 1, \dots, N)$ based on decisions taken by the control unit; (d) finally, any converted packets are routed towards the SF_i $(i = 1, \dots, N)$ where they can reach an output channel.

4.2 MULTISERVICE OCDM/WDM OPTICAL PACKET SWITCH CONTROL ALGORITHM

The scheduling algorithm (SA) is executed at each time-slot of the multiservice OCDM/WDM optical packet switch. The following proposed SA has been modified from [62] in order to support multiservice transmission. The algorithm is composed by three phases; the initialization (IN) phase, in which some sets and parameters are initialized, the code conversion (CC) phase, in which the contention resolution of packets that can be directed without wavelength conversion is resolved by changing the codeword and, finally,

the wavelength conversion (WC) phase, in which packets contentions are resolved by wavelength conversion [92].

The IN phase starts by initializing and introducing some sets and variables. Let $\Lambda_{i,m,j}(i = 1, \dots, N; m = 1, \dots, M; j = 1, \dots, J)$ be the set containing the free output channels in the *i*th OF carried out on the same wavelength λ_m of the J-class system. All these channels are encoded on F different codewords. In addition, let $I_{i,m,j}(i = 1, \dots, N; m = 1, \dots, M; j = 1, \dots, J)$ be the set containing the packets arriving in wavelength λ_m, which are directed to the *i*th OF of the *J*-class system, which are yet to be scheduled. Finally, let R_a denote the available number of wavelength converters, initialized as R and decremented by one each time a converter is used [92]. Both $\Lambda_{i,m,j}$ and $I_{i,m,j}$ are updated during the execution of the SA when the packets are scheduled. After the IN phase, the control unit performs the packet scheduling operations. Next, in the CC phase, for each wavelength $\lambda_m(m = 1, \dots, M)$ the control unit randomly schedules up to F packets of the J-class system, chosen among the packets arriving on wavelength λ_m. The set $\Lambda_{i,m,j}$ initially contains all the output channels in wavelength λ_m and codewords $c_{f,j}(f = 1, \dots, F; j = 1, \dots, J)$ which are used to forward (without wavelength conversion) up to F packets that belong to the $I_{i,m,j}$ set. The following actions are performed by the control unit for each wavelength λ_m [92]: (a) one packet b is randomly selected from the set $I_{i,m,j}$; (b) one output channel $(i, \lambda_m, c_{f,j})$ that belongs to the same *j*th class of the packet b is selected from the set $\Lambda_{i,m,j}$; (c) the packet is scheduled to be forwarded on the output channel $(i, \lambda_m, c_{f,j})$; (d) both the sets $I_{i,m,j}$ and $\Lambda_{i,m,j}$ are updated by removing the elements b and $(i, \lambda_m, c_{f,j})$, respectively.

Finally, in the WC phase the control unit tries to forward with wavelength conversions the remaining packets to the output channels not used in the CC phase. The packets not scheduled as well as the free output channels are stored in I_i and Λ_i, respectively. The following operations are performed by the control unit until either I_i or Λ_i are empty [92]: (a) one packet b is randomly selected from the set I_i; (b) one output channel $(i, \lambda_m, c_{f,j})$ that belongs to the same *j*th class of the selected packet b is selected from the set Λ_i; (c) the packet is scheduled to be forwarded to the output channel $(i, \lambda_m, c_{f,j})$; (d) both sets I_i and Λ_i are updated by removing the elements b and $(i, \lambda_m, c_{f,j})$, respectively; (e) the available number R_a of WC is decremented by one. Before the end of the WC phase, the control unit checks out if there are packets in I_i, and if it is the case they are discarded.

4.3 MULTISERVICE OCDM/WDM OPTICAL PACKET SWITCH PERFORMANCE ANALYSES

In order to evaluate the PLP of the proposed multiservice switch, the BER of the *J*-class MWML-OOC-based OCDM system is required. The BER expression is derived assuming that the MAI has a binomial distribution, since, as it has discussed earlier, the output interference of any OCDMA system is considered to be binomially distributed [50], [58], [84]. Moreover, the MAI is assumed as the only degrading factor of the system. Note that the fiber impairments are ignored here since the main objective is to emphasize the multiservice features of the proposed switch. In addition, it is assumed a chip synchronous scenario, which reflects the worst possible case for the system analysis [50], [84]. Thus, considering also an equiprobable data the BER of class j' users can be obtained as follows [92]

$$BER(j') = \frac{1}{2}\sum_{i=\mu}^{F-1}\binom{F-1}{i}\mathcal{P}^{i}(1-\mathcal{P})^{F-1-i}, \tag{32}$$

where $\mathcal{P}$ is the multiservice multirate probability of interference defined as $\mathcal{P} = \sum_{j=1}^{J} N_j\, p_{jj'}/(F-1)$ [84], and μ is the threshold value of the decision device. N_j is the number of interfering users in class j, and $p_{jj'}$ is the probability of interference caused by a single code of class j on a code of class j', and is written as $p_{jj'} = W_j W_{j'}/2\,L_j$ [58]. For the case of a single-rate system, the probability of interference reduces to $p_{j'j'} = W^2/2L$ *[58]*, where $W = W_{j'}$ and $L = L_{j'}$. It should be mentioned that the user code of class j with W_j chips out of L_j have pulsed signal and can hit on any of the $W_{j'}$ chips of the class j' users [1] Also, the term ½ results from the equal probability of each user transmitting ON-OFF pulses with OOK modulation [92].

Next, it is calculated the PLP of the system considering that interfering users transmit bit "0" and "1" with equal probability ½. In addition, let's consider p as the traffic offered to each input channel, and H as the packet length. As the operation mode of the multiservice switch is synchronous, i.e., the transported packets of each OCDM codeword are synchronized, the PLP is evaluated by conditioning it to the number i of packets that arrive

on any input wavelength transported by *F* distinct codewords [93]. Therefore, the PLP can be expressed as [62], [92]

$$PLP = \sum_{i=2}^{F} \binom{F}{i} p^i (1-p)^{F-i} \; . \; \{1 - \; [1 - BER(i)]^H \}, \tag{33}$$

4.4 MULTISERVICE OCDM/WDM OPTICAL PACKET SWITCH NUMERICAL RESULTS

In this section it is investigated the performance of the multiservice OCDM/WDM switch for a two-class system. Thus, let's consider a two-class system with 10 codewords in the high rate class, $F_1 = 10$ and codeword length $L_1 = 600$ (blue solid lines). For the low rate class it is considered 30 codewords, $F_2 = 30$ and codeword length $L_2 = 1200$ (black dotted lines), respectively [92]. Moreover, it is assumed in all simulations a packet length $H = 500$ bytes, and an offered traffic value of either $p = 0.2$ (circles) or $p = 1$ (diamonds).

In Figure 4.2 the PLP is plotted for the two-class system assuming the same value of codeword weight for the classes, i.e., $W_1 = 5$ and $W_2 = 5$. As can be seen, the two classes have almost the same performance, which is due to both classes having equal codeword weights. It can also be seen that the low rate class produces a slightly higher PLP, which is due to the increased probability of interference for the shorter codewords (high rate class) [58]. Moreover, it can be noticed that a better performance is obtained for both classes when the offered traffic is low [92].

Figure 4.3 shows the PLP versus the number of codewords in the low rate class with codewords weight defined as $W_1 = 8$ for high rate class, and $W_2 = 5$ for the low rate class, respectively. One can observe from this figure that the performance of high rate class is a lot better than that of low rate class. This is mainly caused by the higher codeword weight value of this class when compared to the other class.

Next, it is shown in Figure 4.4 the PLP performance for both classes with codeword weight defined as $W_1 = 5$ for high rate class, and $W_2 = 8$ for low rate class, respectively. Note that the codeword weight of the classes has been alternated. Consequently, the low rate class presents for the first time a better performance than the high rate class [92]. This is due

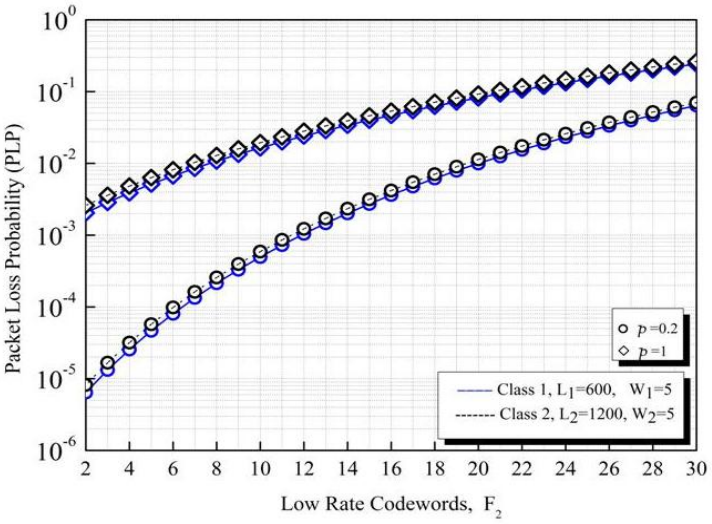

Figure 4.2: PLP as a function of simultaneous users for a two-class system with parameters L_1 = 600, W_1 = 5, L_2 = 1200, and W_2 = 5. The number of interfering users in the class 2 is varied from 2 to 30, and the number of class 1 users is fixed to F_1 = 10. The traffic parameters are H = 500 bytes, and offered traffic of either p = 0.2 or p = 1.

to the higher codeword weight of the former. It is straightforward to figure out that one class outperforms others whenever its codeword weight is higher. On the other hand, the classes will perform approximately the same when their codeword weights are equal. Further, it is worth pointing out that a low traffic p allows a reduction of the MAI and, consequently, an increase in the supported number F of codewords [62].

Finally, note that by decreasing the offered traffic, the PLP is decreased and the performance is improved for both classes in all scenarios. The performance analysis of the switch has shown that a large number of users' codewords from different classes can be transmitted simultaneously with acceptable PLP [92]. It is clear that better performance is obtained either when classes are defined with high-weight codewords or when low traffic is offered.

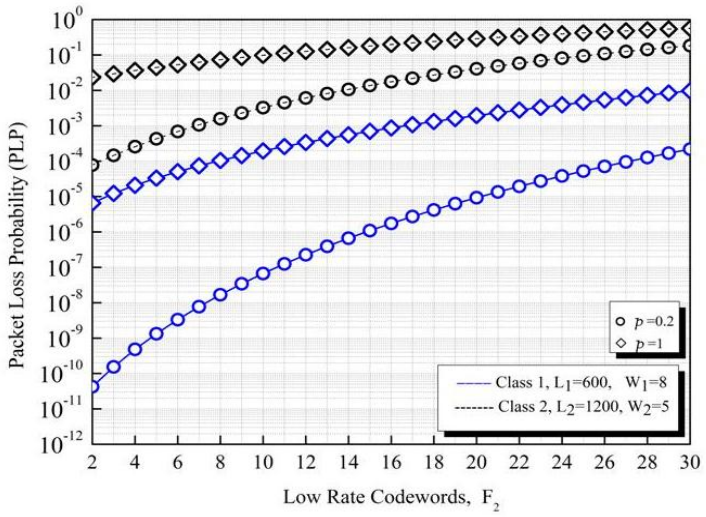

Figure 4.3: PLP as a function of simultaneous users for a two-class system with parameters L_1 = 600, W_1 = 5, L_2 = 1200, and W_2 = 8. The number of interfering users in the class 2 is varied from 2 to 30, and the number of class 1 users is fixed to F_1 = 10. The traffic parameters are H = 500 bytes, and offered traffic of either p = 0.2 or p = 1.

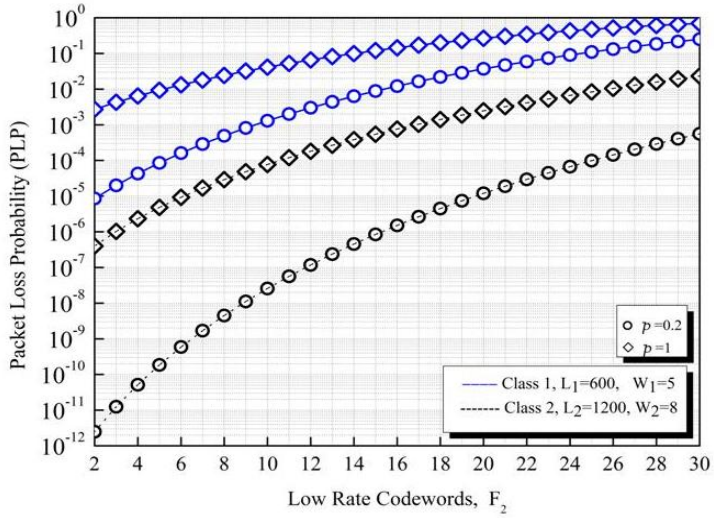

Figure 4.4: PLP as a function of simultaneous users for a two-class system with parameters L_1 = 600, W_1 = 8, L_2 = 1200, and W_2 = 5. The number of interfering users in the class 2 is varied from 2 to 30, and the number of class 1 users is fixed to F_1 = 10. The traffic parameters are H = 500 bytes, and offered traffic of either p = 0.2 or p = 1.

CHAPTER 5

NUMERICAL RESULTS AND DISCUSSIONS

In this chapter, the numerical simulation results obtained with the proposed formalisms described in Chapter 3 are presented and discussed. The block diagram of the multirate, multiservice OCDMA network to be investigated here is schematically shown in Figure 5.1. As depicted in this figure, the data bits' sequences of *U* simultaneous users are converted to optical domain and modulated in OOK format (grey block). In this modulation format, a bit "1" is represented by the presence of an optical pulse while the bit "0" is represented by the absence of optical pulse.

The OCDMA encoder (green block) encodes the optical pulses subdividing them into short chips. A single code sequence is then assigned to each user, where the number of illuminated chip positions is determined by the code weight. After, the sequences assigned to the users should access the transmission channel, which is provided by the passive coupler (light purple circle) illustrated in Figure 5.1. Afterwards, the coded data from all users *U* propagate through the optical channel and then are delivered to each OCDMA decoder by means of decouplers (light purple circle) configured in star topology.

As is well known, only the decoder assigned to the desired user has the sequence required to decode the transmitted data. The transmitted signals from all other users contribute to MAI, the mechanism of interference that can severely affect the overall system performance. The decoded data is then sent to the photodetector (blue block) and finally to the demodulation process (orange block). In spite of the fiber representation in Figure 5.1, all the systems analyzed in this work are considered to be "back to back".

The formalism developed in Chapter 3 is now applied to two distinct multirate, multiservice scenarios employing: 1) a strict 1-D MWML-OOC codes assuming binomial and Poisson distributions for the MAI, and 2) a 2-D OFFH-CDMA system assuming binomial and gaussian distributions for the MAI.

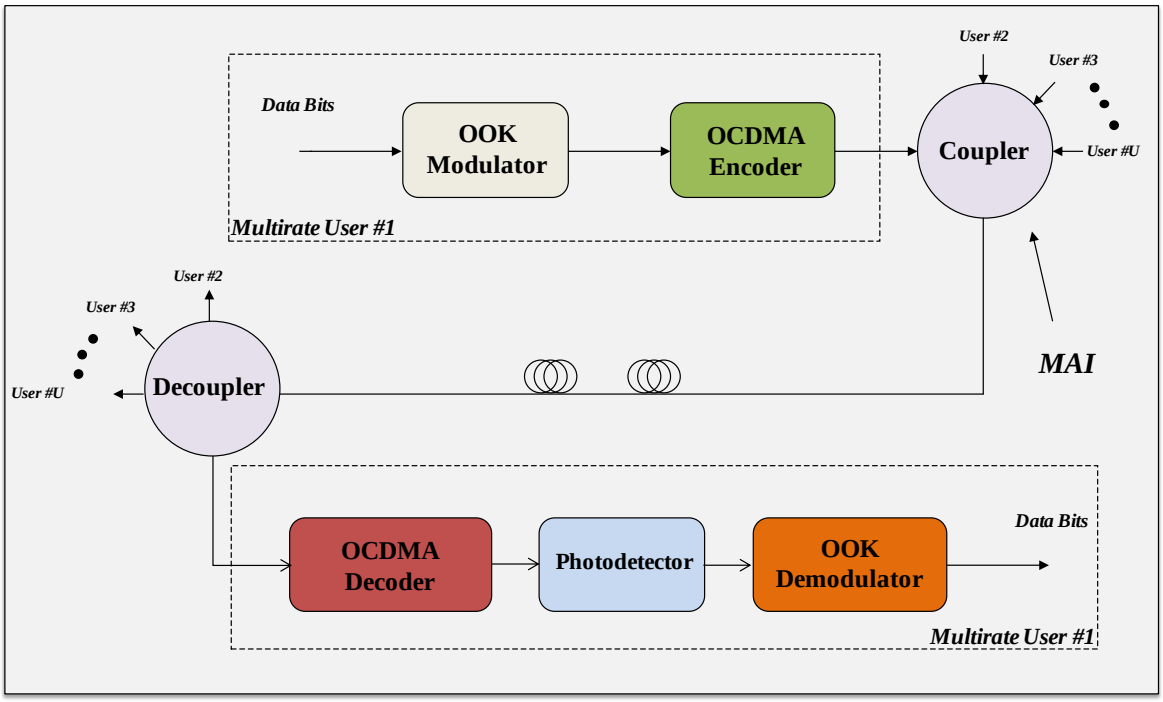

Figure 5.1: Block diagram of the multirate, multiservice OCDMA system.

5.1 MULTIRATE, MULTISERVICE 1-D MWML-OOC OCDMA SYSTEM

The results presented in this section have been obtained with the formalism developed in Chapter 3, Sections 3.13 and 3.15. It is simulated a two-class system with parameters $L_1 = 500$, $W_1 = 5$, and $U_1 = 4$ for the high rate users (squares) and $L_2 = 1500$, $W_2 = 5$, and $U_2 = 20$ for the low rate users (circles), respectively.

The results for BER versus detection threshold considering both binomial and Poisson distributions for the MAI are plotted in Figure 5.2. This comparison is important for validation purposes of the proposed formalism. The curve for Poisson distribution is obtained directly from [58], and shows a good agreement with our proposed formalism, particularly at low threshold values. As can be seen, at higher threshold values ($u > 3$), the curves detach from each other. Note from these results that both users' classes have essentially the same performance, a consequence from being defined with the same code weight and equal code orthogonality between different classes [3]. Also note that for both Poisson (solid lines) and

binomial (dashed lines) distributions, the low rate class produces a BER (circles) a little bit higher than that for high rates (squares), which is a consequence of the increased probability of interference from the high rate class [58]. Hence, the Poisson-based results (solid lines) for this particular multirate scenario are accurate enough.

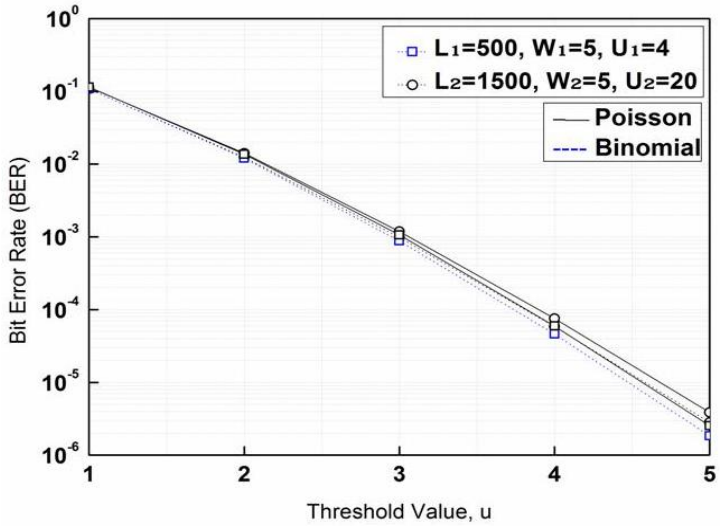

Figure 5.2: BER for a two-class MWML-OOC OCDMA system with equal code weights and different code lengths for both classes. Dotted lines are the binomial approach. Solid lines are the Poisson approach simulation results [58].

Next, we carry on the validation procedure a step further and investigate the BER versus the number of users for three different users' classes, $J = 3$. The code length, weight, and number of users respective to the three classes are, $L_1 = 500$, $W_1 = 7$, and $U_1 = 4$ (diamonds), $L_2 = 1000$, $W_2 = 5$, and $U_2 = 20$ (squares), and $L_3 = 1500$, $W_3 = 3$, and $U_3 = 20$ (circles) (the subscripts 1, 2 and 3 refer to the three different classes). Furthermore, the optimum threshold value was set to the respectively user's code weight of each class. Also, the frequency parameter F is set to 1 (see equation (11)) since this is a 1-D system. Note that the users' transmission rates are transparent to the formalism and are accounted for in terms of the code length ratio between the involved classes.

The results obtained with the Poisson (solid lines) and the proposed binomial (dashed lines) approaches are shown in Figure 5.3. It is important to stress at this point that the curve corresponding to the binomial approach agrees quite well with the one from [58], obtained using the Monte Carlo simulation method (and assumed here as exact). Therefore, it can be concluded from these results that the present approach produces more accurate results for the

MAI than does the Poisson distribution [8], [58]. Class 3 (the lowest rate class) shows inferior BER performance (QoS) of all three classes in the system, which is basically due to its lowest code weight. Moreover, increasing the number of users in class 3 will barely modify the overall system performance, since this class has the lowest code weight as well as the largest code length, leading to a very low probability of interference caused by this class.

These results also show that the overall performance of this multirate, multiclass system is so poor that none of the users' classes can operate even at the standard BER scenario ($BER < 10^{-9}$). For instance, class 3 (low rate, and low QoS user class) produces a BER on the order of 1×10^{-3} (circles), while class 2 (medium rate, and medium QoS user class) produces a BER of about 4.5×10^{-5}. Both of these BER values are extremely high, so much so that even a forward error correction (FEC) algorithm is not able to reduce it to acceptable levels [50]. It is worth mentioning that for BER levels of at the most 1×10^{-5}, FEC algorithms such as Reed-Solomon RS(255,223) can reduce the BER down to the error-free zone around 1×10^{-12}. Observe in Figure 5.3 that only class 1 (high rate, and high QoS user class) could attain error-free operation with such a FEC technique. Therefore, additional techniques to mitigate MAI are of paramount importance in multirate systems.

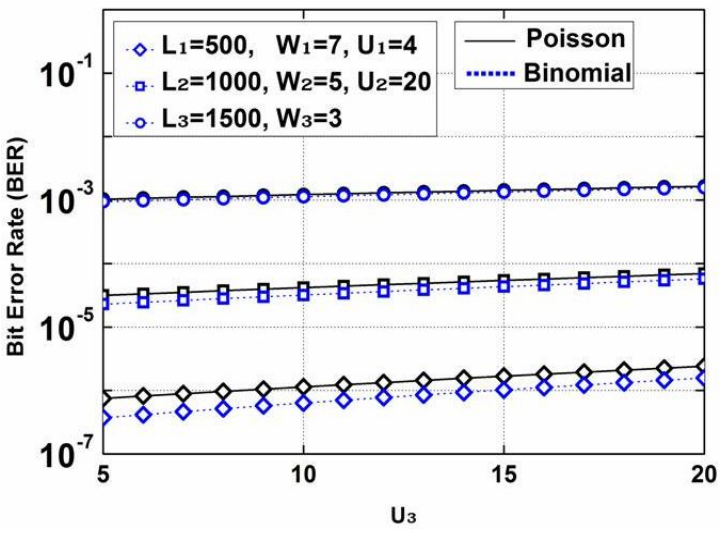

Figure 5.3: BER as a function of simultaneous users for a three classes MWML-OOC system. The MAI distributions are Poisson (solid lines) [58] and binomial (dotted lines) [8]. The subscripts 1, 2 and 3 refer to the different classes investigated.

Next, we carry out a system performance comparison between the two BER approaches for a three-class MWML-OOC OCDMA system, as shown in Figure 5.4. The following parameters were considered in the simulations: $L_1 = 600$, $W_1 = 5$, and $U_1 = 2$ for

the lowest rate class, $L_2 = 400$, $W_2 = 3$, and $U_2 = 10$ for the medium rate class, and $L_3 = 200$, $W_3 = 1$, and $U_3 = 10$ for the highest rate class. Further, the optimum threshold value was set to the respective user's code weight of each class, and the frequency parameter F was set to 1 in expression (11), since this is a 1-D system.

It can be observed from this figure that the Poisson approximation can be satisfactorily applied to this multirate scenario as it tends towards the binomial one for all three classes. Observe also that for class 1, both Poisson and binomial approximations produce identical results (diamonds). Nonetheless, the BER of class 3 is severely affected because of the lowest code weight attributed to the class in this multirate, multiservice system, as shown in Figure 5.4.

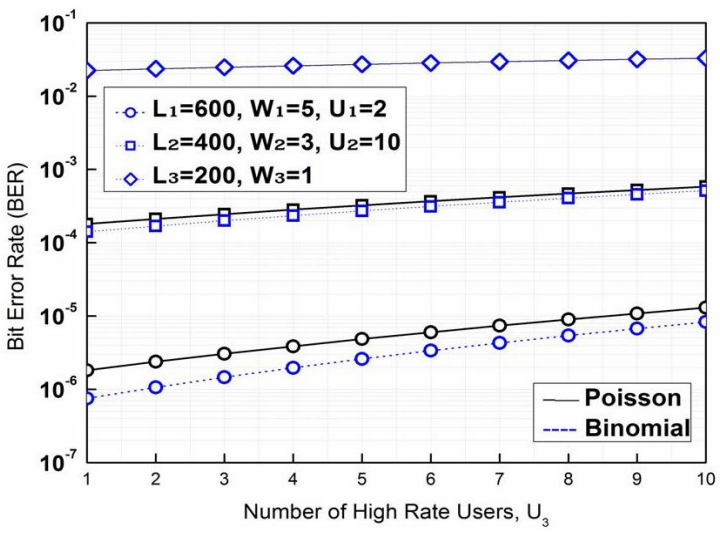

Figure 5.4: BER performance for a three-class system with parameters L1 = 600, W1 = 5, and U1 =2, L2 = 400, W2 = 3, and U2 = 10, L3 = 200, W3 = 1, and U3 = 10. The subscripts 1, 2 and 3 refer to the different classes investigated. The number of users in the third class is varied from 1 to 10. Binomial approach (dashed lines) and Poisson approximation (solid lines).

Now, the same three-class system described above is considered again, but with different simulation parameters. The idea is to show that the Poisson approach may lead to misleading BER results for some 1-D MWML-OOC OCDMA multirate, multiservice scenarios. The following parameters are used: $L_1 = 500$, $W_1 = 6$, and $U_1 = 2$ for the high rate class, $L_2 = 1500$, $W_2 = 3$, and $U_2 = 28$ for the low rate class, and $L_3 = 1000$, $W_3 = 9$, and $U_3 = 2$ for the medium rate class.

The results for all three classes are shown in Figure 5.5. It can be observed from Figure 5.5 that for 10 active users in class 2, $U_2 = 10$, there will be a total of 14 simultaneous

users present in the system. In other words, there are 2 users in class 1 (high rate, medium QoS class), 10 users in class 2 (low rate, low QoS class) and 2 users in class 3 (medium rate, high QoS class), totaling 14 simultaneous users.

One can further observe from this figure that as the number of simultaneous users decreases, the binomial-based BER curve drops more rapidly than that obtained with Poisson. When the number of users is not large enough the Poisson-based BER diverges significantly from the binomial one, thus resulting in a really poor approximation as can be seen in the figure. For instance, if an error-free scenario is desirable, i.e., $BER < 10^{-12}$, (see horizontal dashed line in Figure 5.5) the BER curve representing the Poisson approach underestimates the number of simultaneous users in class 2 by 53%. For the case of a standard BER scenario, i.e., $BER < 10^{-9}$, the Poisson-based BER predicts about 62% less users in class 2 than the binomial-based BER. Therefore, for this case it can be concluded that only the binomial-based BER can be considered precise enough to evaluate accurately the BER performance of the system.

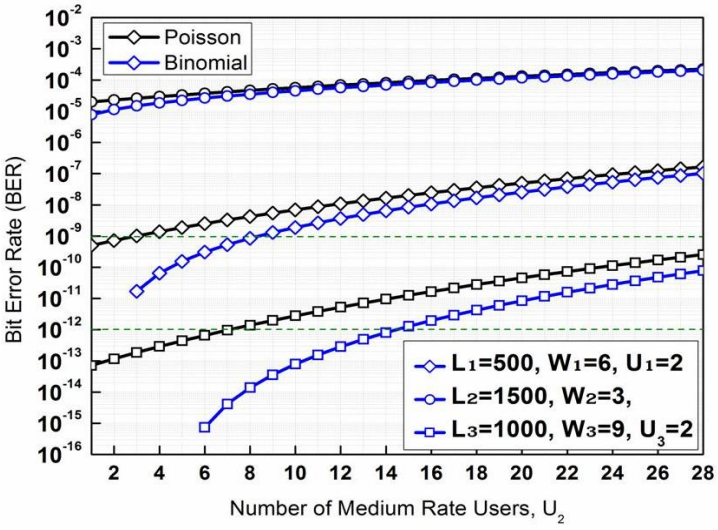

Figure 5.5: BER for the lowest rate users' class with L3 = 2000, W3 = 13, and U3 = 4. The subscripts 1, 2 and 3 refer to the different classes investigated. The number of users in the second class is varied from 6 to 120. The MAI distributions are Poisson (solid line) and binomial (dotted line).

The next three-class MWML-OOC OCDMA system to be considered presents the following parameters: $L_1 = 500$, $W_1 = 7$, and $U_1 = 4$ for the high rate class, $L_2 = 1500$, $W_2 = 3$, and $U_2 = 120$ for the medium rate class, and $L_3 = 2000$, $W_3 = 13$, and $U_3 = 4$ for the low rate class. Also, the optimum threshold value was set to the respectively user's code weight

of each class. The main idea here is to determine how many users should be on the system so that Poisson can accurately approximate a binomial distribution.

Figure 5.6 shows the BER performance comparison results between the two distributions, but only for the low rate users' class. As in the previous example, as the number of simultaneous users decreases, the BER curve with binomial distribution (dashed-line) drops more rapidly than that obtained with Poisson distribution (solid-line). The difference between both approaches becomes more dramatic particularly if an error-free scenario is desirable ($BER < 10^{-12}$, see horizontal dotted-line in Figure 5.6). In such case, the BER curve with Poisson underestimates the number of users in 33% when compared to the binomial case. A satisfactory convergence between both approaches will only occur when more than 70 simultaneous users are present in the system (see vertical dotted-line in Figure 5.6) [8]. Observe also that even for a standard BER scenario, i.e., $BER = 10^{-9}$, the Poisson-based BER predicts about 12% less users than the binomial-based BER. Therefore, for this multirate scenario, the Poisson distribution is also not very accurate for a good BER performance estimation.

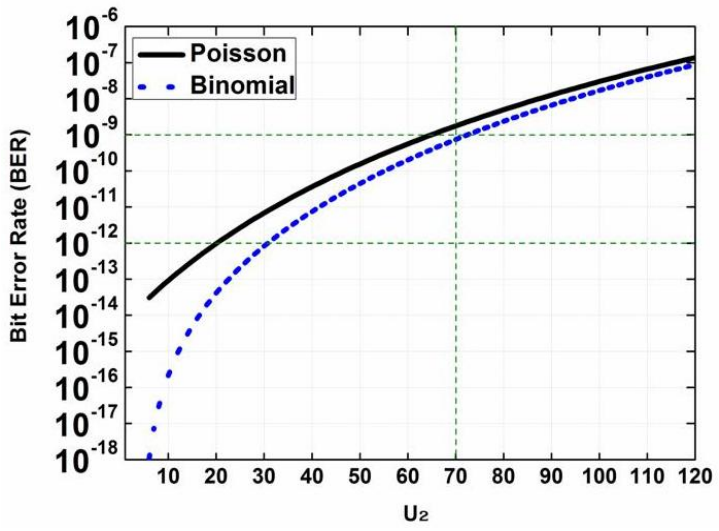

Figure 5.6: BER for the lowest rate users' class with $L_3 = 2000$, $W_3 = 13$, and $U_3 = 4$. The subscripts 1, 2 and 3 refer to the different classes investigated. The number of users in the second class is varied from 6 to 120. The MAI distributions are Poisson (solid line) and binomial (dotted line).

5.2 MULTIRATE 2-D OFFH-CDMA SYSTEM

The results presented in this section have been obtained with the formalism developed in Chapter 3, Section 3.12 and 3.13. It is considered a two-class system with the following code length, code weight and number of users respective to the three classes: L_1 = *12*, W_1 =*12*, and U_1 = *17* for the low rate users (class 1, circles) and L_2 = *6*, W_2 =*6*, and U_2 = *6* for the high rate users (class 2, diamonds). The code sequences of all users in the system share the same number of available wavelengths, with *F = 29*. It is worth saying that 29 wavelengths can provide at most 29 code sequences [80].

Moreover, the transmission rate magnitude of the users is transparent to the formalism and is accounted for by means of the code length ratio between the classes of the system. Even though the formalism employed in the simulations assumes MAI as the only noise source, it equally allows the possibility of including other noise sources [50], as well as mechanisms to mitigate their influence, such as FEC.

Figure 5.7 plots the BER versus threshold level for both classes. As can be seen, the BER is minimized when the threshold level equals the code weight of the desired user in consideration, i.e., at μ_{opt_1} = *12* (class 1) and μ_{opt_2} = *6* (class 2). Even though the threshold is taken as equal to the code weight, note that the formalism presented in Chapter 3, Section 3.1 provides a more general choice of threshold values by treating the threshold as a free parameter to be chosen optimally. This is possible since the threshold value in the BER expression (11) can be set to any value, not necessarily the optimum one. As a matter of fact, the optimal threshold cannot always be taken as equal to the weight, even when the MAI is considered as the only degrading factor of the system [48]. Although in most works the decision threshold value used in the users' detector may be set to the code weight (ensuring that no decision error will be made when a bit “1” is sent, when the channel is ideal), in [48] it is reported that this adjustment works well when the MAI is small compared to the code weight. When this is not the case, the probability of error associated with a data bit “0” increases when the average interference power in the optical channel is high. This can be remedied by increasing the threshold value beyond the code weight. Further, it might be of absolute interest to consider a general choice of threshold by treating the threshold value as a free parameter to be chosen optimally.

Before we proceed any further with the analysis of this multirate/multiclass scenario, some additional explanations become necessary. As we have mentioned throughout this

dissertation, we have assumed the worst case scenario for the system simulation, i.e., chip synchronization and one chip coincidence for any user once that the exact performance depends on which codes are interfering on the desired user code. This requires consequently an exact knowledge of the actual interference patterns (probability density functions (PDFs)).

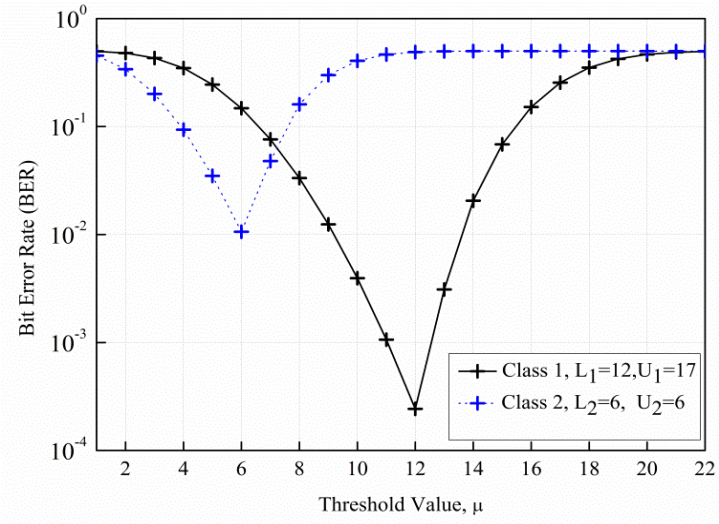

Figure 5.7: Optimum detection threshold with L_1 = 12, L_2 = 6, U_1 = 17, U_2 = 6, and F = 29. The BER of high rate users and low rate users are minimized by choosing threshold values of 6 and 12, respectively.

Unfortunately, this also requires an exact calculation of all interference patterns (considering *U* as the total number of users, there will be *U (U-1) / 2* interference patterns) which would be computationally and mathematically costly. Fortunately, one can bound the effects (means and variances) of these interference patterns by their worst case, namely, chip synchronous and one chip coincidence (each interfering user contributes with one chip to overlapping), when there are only two users transmitting data simultaneously in the system. When more than two users are simultaneously present, the interference (measured as the mean and variance of the signal) of each interfering user with respect to the desired user becomes the same. Since each interfering signal is identical and an independent random variable, the mean and variance of the total interference signal can be expressed as the product of each mean and variance of the interfering signal.

Furthermore, it is well known from statistics theory that in order to obtain a really good gaussian estimation, the number of trials N_j (number of interfering users) should be large enough, and the probability of interference as possible as close to 0.5 [55], [86], [94]. As will be show below, for a system in which the number of users is not large enough the

gaussian approximation is not appropriate to an accurate evaluation of the system performance.

With that in mind, let's now proceed with the comparison analysis between gaussian and binomial distributions given in terms of BER versus number of users in class 1, as shown in Figure 5.8. In the simulations were used equation (17) with its right hand side term equals zero. This figure shows that the BER of the high rate class 2 (diamonds solid line) is more severely affected by MAI than that for the low rate class 1 (circles solid line). This is due to the smaller code weight of class 2 when compared to class 1 [53], [84].

One can also note from this figure that as the number of simultaneous users decreases, the gaussian-based BER curve drops more rapidly than that obtained with binomial distribution. Moreover, the approximated results for class 2 (diamonds dashed line) is more accurate than those for class 1 (circles dashed line), which is due to the smaller threshold value ($\mu_{opt_2} = 6$) of the former [55]. Observe that the gaussian based-BER underestimates the system performance in unacceptable levels, and incorrectly predicts the number of simultaneous users for any given BER. This suggests that the gaussian based-BER is not appropriate for a reliable BER estimate in the present multirate OFFH system. Consequently, the binomial BER-based approach must be used to correctly predict the system performance for any number of users in the presented system.

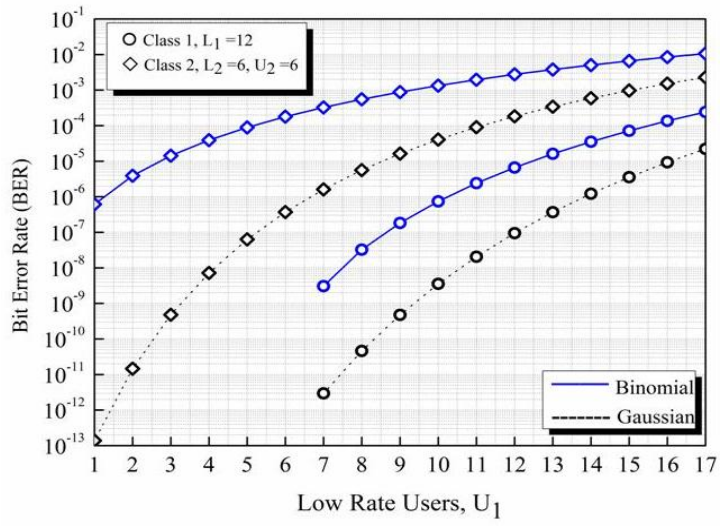

Figure 5.8: BER performance for a two-class system with parameters L_1=12, L_2=6, and F=29. The number of users in Class 1 is varied from 1 to 17. Binomial approach (solid lines) and gaussian approximation (dashed lines) [84].

Observe in Figure 5.8 that the curves for class 1 (circles lines) start with a number of simultaneous users above the code weight W_1 plus one ($W_1 + 1$). It means that it is necessary at least $W_1 + 1$ simultaneous users in the system for errors start occurring. This happens because of MAI is the only degrading factor of the system being considered, the detection threshold is set to the code weight W_1, and the codes adopted in the system have good auto- and cross-correlation properties. For instance, considering $W_1 = 12$ in Figure 5.8, errors begin to occur only at $U_1 = 7$ plus $U_2 = 6$, which means that before this point there are no errors for users of class 1. The same concept is valid for class 2, where errors begin to occur only when the number of simultaneous users is above $W_2 + 1$. For instance, considering $W_2 = 6$ in Figure 5.8, errors begin to occur at $U_1 = 1$, since there are already 6 fixed users from class 2 ($U_2 = 6$), totaling 7 simultaneous users.

In the next example, the previous two-class system is again investigated but this time with a smaller number of users in class 2, i.e., $U_2 = 4$. The main idea is to analyze the behavior of the gaussian approximation at a condition where it is expected to fail and compare it with the proposed binomial approximation. The results shown in Figure 5.9 clearly demonstrate that the gaussian approximation indeed performs very poorly at this condition, as one should expect. In fact, the only evident change is in the position where errors start occurring.

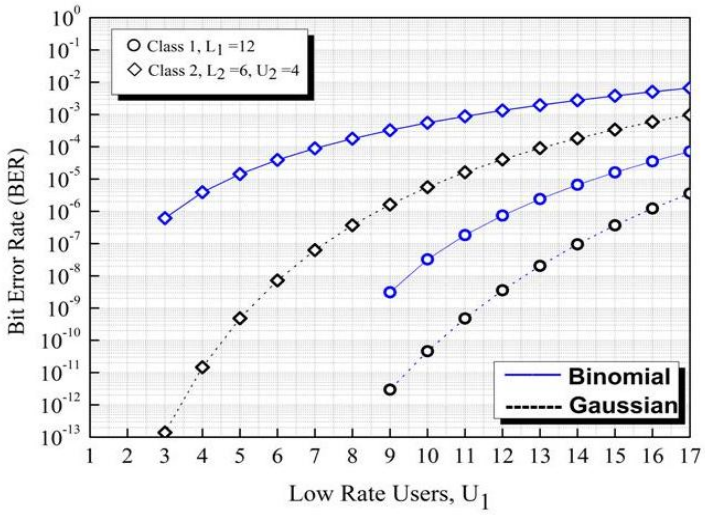

Figure 5.9: BER performance for a two-class system with parameters $L_1 = 12$, $L_2 = 6$, and $F = 29$. The number of users in Class 1 is varied from 1 to 17. Class 2 has only 4 users, $U_2 = 4$. Binomial approach (solid lines) and gaussian approximation (dashed lines).

The lower number of users in class 2 (in the previous example $U_2 = 6$) decreases the overall MAI contribution and therefore allows for a larger number of users in the other class. This can also be seen as a simple way to allocate more users in that class if the demand for that transmission rate increases. For instance, in Figure 5.8 the number of simultaneous users in class 1 for $BER = 10^{-9}$ is about 9 (dashed line, circles), while in Figure 5.9 it is 11 (dashed line, circles). Even though these results appear consistent with what one would expect, the inaccuracy in predicting the BER and number of active users (when compared to the binomial approach) makes the gaussian approach completely inadequate for this task.

Finally, for the sake of clearness, we replot in Figure 5.10 the BER versus low rate users from Figures 5.8 and 5.9, but just for the proposed binomial approach. Observe that the system performance for both classes changes noticeably, even though the number of active users in both high rate classes 2 is not very different. In addition, note that the presence of just two more users in the high rate class 2 ($U_2 = 6$, solid line) is enough to change the BER by nearly one order of magnitude for most users in class 1 (compare with $U_2 = 4$, dashed line), consequently reducing the number of active low rate users. Therefore, one can conclude from this analysis that increasing the number of high rate users causes a tremendous deleterious impact in multirate OFFH systems. Nonetheless, acceptable levels of BER can still be successfully achieved in these systems by means of MAI mitigation mechanisms and FEC techniques.

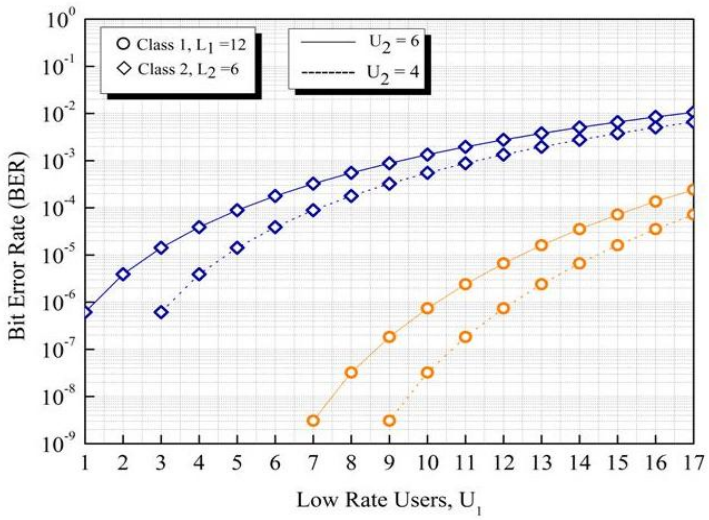

Figure 5.10: BER performance for a two-class system with parameters $L_1 = 12$, $L_2 = 6$, and $F = 29$. The number of users in Class 1 is varied from 1 to 17. The number of users in class 2 is either $U_2 = 4$ or $U_2 = 6$.

CHAPTER 6

CONCLUSION

In this dissertation, it has been proposed a new approach for evaluating the BER of multirate, multiservice OCDMA systems. The new and more accurate BER expression for multirate, multiservice systems is based on binomial distribution for the MAI. All analysis performed in this work considered the MAI as the only source of noise, since the major objective was to analyze the system performance considering scenarios in which different classes of users transmit with different data rates or quality of service (QoS).

Furthermore, the performance of multirate, multiservice OCDMA systems employing 1-D and 2-D codes has been investigated. In systems employing 1-D codes it was utilized the so-called MWML-OOC, a strict multi-weight multi-length code specifically proposed for multiservice systems. The proposed formalism can be successfully deployed in most multi-weight, multi-length family of codes as long as the corresponding code parameters are used. In systems employing 2-D codes it was utilized the so-called OFFH-based code. This sort of code is classified into the category called one-coincidence sequences due to its intrinsic properties. It is worth to mention that the correlation properties of both of these code families are bounded by one at maximum. The performance of the systems was investigated using only the parameters of the codes adopted in the analysis, once that the approach proposed here does not require the generated code sequences themselves. The systems investigated were considered as back-to-back. It was also assumed chip synchronous scenarios, which reflects the worst case for the system analysis and on-off keying (OOK) as the modulation format.

Numerical simulation results proved that the multirate OCDMA systems based on MWML-OOC and OFFH codes are not capable of accommodating a large number of users in an error-free environment, i.e., $BER<10^{-12}$, unless forward error correction (FEC) techniques are used as well. The results further demonstrated that users' class of high rate transmission in the multirate OFFH-CDMA system presents worse performance than users of low rate class.

This happened due to the lower code weight of high rate user's class when compared to the low rate user's class. This occurs since in OFFH-based codes the weight is equal to the code length itself which does not allow manipulation of the BER or QoS performance without changing the transmission rate together. On the other hand, it was shown in the MWML-OOC OCDMA system that users' class can have high rate transmission and excellent BER performance at the same time. This is possible because the code employed in this multirate system can be manipulated with more freedom. More specifically, the code weight does not necessarily have to be equal the code length like in OFFH-based codes. Thus, this allows the configuration of users classes with different data rates and QoS.

It was also carried out a performance comparison in terms of BER for the MWML-OOC-based system assuming both Poisson and binomial distribution for the MAI. Similarly, a comparison for the OFFH-based system assuming both gaussian and binomial distribution for the MAI was also carried out. It was shown that BER performance in multirate scenarios can be overestimated or underestimated by many orders of magnitude depending on the assumed distribution for the MAI and on the number of simultaneous users. For a small number of users the Poisson distribution does not provide a reliable approximation to evaluate the system BER performance in many multirate scenarios. Moreover, the Poisson assumption underestimates the number of simultaneous users in the system.

It could also be observed that the approximated BER is more accurate for the users classes with smaller threshold values, meaning also that users classes with lower BER performance present more accurate results. Also it is noted that the gaussian-based BER underestimates the system performance in unacceptable levels, and overestimates the number of simultaneous users on the system. And when a low number of users are present, neither gaussian nor Poisson distribution is a good approximation to assess the BER performance of multirate systems with acceptable accuracy.

Finally, it was demonstrated for the first time a hybrid OCDM/WDM optical packet switch capable of supporting multirate and differentiated-QoS transmission. In order to provide multiple rates and differentiated-QoS, it was employed MWML-OOC as user signature codeword of an incoherent OCDM scheme. The architecture of the proposed multirate switch and its performance in terms of packet loss probability (PLP) have also been presented. The results have shown that the proposed switch can accommodate a considerably large number of users from different classes with acceptable PLP. Also, employing low offered traffic in hybrid systems allows an increase in the number of users supported under a

given PLP. It was shown that a given user's class performs better when its weight is higher than the weight defined for the codewords of the other user's class. In addition, all the system's classes perform reasonably equally when the codeword weight of classes are defined as the same.

REFERENCES

[1] H. Beyranvand, B. M. Ghaffari, and J. A. Salehi, "Multirate, differentiated-QoS, and multilevel fiber-optic CDMA system via optical logic gate elements," IEEE J. Lightwave Technol., vol. 27, no. 19, pp. 4348–4359, Oct. 2009.

[2] F. Farnoud, M. Ibrahimi, and J. A. Salehi, "A packet-based photonic label switching router for a multirate all-optical CDMA-based GMPLS switch," IEEE J. Sel. Topic Quantum Electron., vol. 13, no. 5, pp. 1522–1530, Sep. 2007.

[3] S. V. Maric, O. Moreno, and C. J. Corrada, "Multimedia transmission in fiber optical LANs using optical CDMA," IEEE J. Lightwave Technol., vol. 14, no. 10, pp. 2149-2153, Oct. 1996.

[4] J. G. Zhang, "Flexible optical CDMA networks using strict optical orthogonal codes for multimedia broadcasting and distribution applications," IEEE Trans. Broadcast., vol. 45, pp. 106–115, Mar. 1999.

[5] M. Menif, P. Gallion, C. Karaborni, and H. Rezig, "Performance evaluation for a new implementation of multirate optical fast frequency hopping CDMA system for multimedia transmission," Electronics, Circuits and Systems, 2005. ICECS 2005. 12th IEEE International Conference on , vol., no., pp.1-4, 11-14, Dec. 2005.

[6] M. Thiruchelvi, M. Meenakshi, and G. Geeth, "Multimedia applications using optical FFH-CDMA communication system," IEEE, Microwave and optical technology letters, Vol. 34, N°.4, August 2002.

[7] E. Inaty, H. M. H. Shalaby, and P. Fortier, "A new transmitter-receiver architecture for noncoherent multirate OFFH-CDMA system with fixed optimal detection threshold," J. Lightwave Technol., vol. 20, no. 11, pp. 1885–1894, Nov. 2002.

[8] T. R. Raddo, A. Sanches, J. V. dos Reis Jr., and B. V. Borges, "Influence of the MAI distribution over the BER evaluation in a multirate, multiclass OOC-OCDMA system," in Access Networks and In- House Communications (ANIC), OSA, paper ATuB5, 2011.

[9] T. Koonen, "Fiber to the home/fiber to the premises: What where and when?," Proceedings of the IEEE, vol. 94, no. 5, pp. 911--934, Invited Paper, May 2006.

[10] C.-H. Lee, "Passive Optical Networks for FTTx Applications," Optical Fiber Communication Conference, pp. 3-, vol. 3, Mar. 2005.

[11] C. Lee, W. V. Sorin, and B. Y. Kim, "Fiber to the Home Using a PON Infrastructure," J. Lightwave Technol. 24, 4568-4583, 2006.

[12] R.-N., T. Roth, R. Ram, R. Kirchain, R., "Characterizing the Capex and OpEx Tradeoffs in Next Generation Fiber-to-the-Home Networks," Optical Fiber communication/National Fiber Optic Engineers Conference, pp. 1-3, Feb. 2008.

[13] J. V. dos Reis, Jr., "Modelagem de erros CDMA-PON baseadas em técnicas de cancelamento paralelo e códigos corretores de erros," Dissertation submitted for the degree of Master of Science at University of São Paulo (USP), São Carlos School of Engineering, 2009 (in Portuguese).

[14] H. Lundqvist, "Error Correction Coding for Optical CDMA," Thesis submitted to KTH, The Royal Institute of Technology, 2003.

[15] M. M. Karbassian, "Design and analysis of spreading code and transceiver architectures for optical CDMA networks," Thesis submitted for the degree of Doctor of Philosophy at University of Birmingham, 2009.

[16] N. Kheder, "Experimental Demonstration of CDMA and OTDMA PONs with FEC and Burst-Mode," Thesis submitted for the degree of Master at McGill University, Feb. to McGill University, 2008.

[17] A. R. Dhaini, P.-H. Ho, G. Shen, "Toward green next generation passive optical networks," Communications Magazine, IEEE, vo1.49, no. 11, pp. 94-101, November 2011.

[18] M. de Andrade, M. Tornatore, S. Sallent, and B. Mukherjee, "Optimizing the migration to future-generation passive optical networks (PON)," IEEE Syst. J., vol. 4, no. 4, pp. 413–423, Dec. 2010.

[19] R. Davey, J. Kani, F. Bourgart, and K.McCammon, "Options for future optical access networks," IEEE Commun. Mag., vol. 44, no. 10, pp. 50–56, Oct. 2006.

[20] H.-Y. Tyan, J. C. Hou, B. Wang, and C.-C. Han, "On supporting temporal quality of service in WDMA-based star-coupled optical networks," IEEE Trans. Comput., vol. 50, no. 3, pp. 197–214, Mar. 2001.

[21] H. Yin and D. Richardson, Optical code division multiple access communication networks: theory and applications. Tsinghua University Press, Springer-Verlag, 2008.

[22] P. R. Prucnal, Optical Code Division Multiple Access: Fundamentals and Applications. New York: Taylor & Francis, Dec. 2005.

[23] K. Fouli and M. Maier, "OCDMA and Optical Coding: Principles, Applications, and Challenges," IEEE Commun. Mag., vol. 45, no. 8, pp. 27-34, Aug. 2007.

[24] A. Stok and E. H. Sargent, "The role of optical CDMA in access networks," IEEE Commun. Mag., vol. 40, no. 9, pp. 83–87, Sep. 2002.

[25] C. F. Zhang, K. Qiu and B. Xu, "Multiple-access technology based on optical code-division multiple access for passive optical networks," Opt. Eng., pp. 105002.1.105002.5, 2006.

[26] H. Beyranvand, J. A. Salehi, "Multirate and Multi-Quality-of-Service Passive Optical Network based on Hybrid WDM/OCDM System," IEEE Communications Magazine, vol. 49, pp. 39-44, 2011.

[27] H. Beyranvand and J. A. Salehi, "Multiservice Provisioning and Quality of Service Guarantee in WDM Optical Code Switched GMPLS Core Networks," journal of Lightwave Technology, vol. 27, no. 12, pp. 1754-1762, 2009.

[28] H. Beyranvand and J. A. Salehi, "All-Optical Multi-Service Path Switching in Optical Code Switched GMPLS Core Network," IEEE J. Lightwave Tech., vol. 27, no. 12, pp. 2001–12, June 2009.

[29] W. Chung, J. Salehi, and V. Wei, "Optical orthogonal codes: Design, analysis, and applications," IEEE Trans. Inform. Theory, vol. 35, no. 3, pp. 595-604, May 1989.

[30] J. Salehi, "Code division multiple-access techniques in optical fiber networks - Part I: Fundamental principles," IEEE Trans. Commun., vol. 37, no. 8, pp. 824-833, Aug. 1989.

[31] J. Salehi and C. A. Brackett, "Code division multiple-access techniques in optical fiber networks - Part 2: Systems performance analysis," IEEE Trans. Commun., vol. 37, no. 8, pp. 834-842, Aug. 1989.

[32] S. Mashhadi and J. A. Salehi, "Code division multiple-access techniques in optical fiber networks—part III: optical AND gate receiver structure with generalized optical orthogonal codes," IEEE Trans. Commun., vol. 45, pp. 1457-1468, Aug. 2006.

[33] X. Wang and K. Kitayama, "Analysis of beat noise in coherent and incoherent time-spreading OCDMA network," J. Lightwave Technol., vol. 22, no. 10, pp. 2226–2235, Oct. 2004.

[34] S. Yoshima, Y. Tanaka, N. Kataoka, N. Wada, J. Nakagawa, and K. Kitayama, "Full-duplex 10G-TDMOCDMA-PON system using only a pair of en/decoder," ECOC 2010, Tu.3.B.6, Torino, Italy, Sep. 2010.

[35] X. Wang, N. Wada, T. Miyazaki, G. Cincotti, and K. Kitayama, "Hybrid WDM/OCDMA for next generation access network," Proc. SPIE 6783, 678328, 678328-14, 2007.

[36] M. Gharaei, C. Lepers, O. Affes, and P. Gallion, "Teletraffic capacity performance of WDM/DS-OCDMA passive optical network," NEW2AN/ruSMART 2009, LNCS 5764, Springer-Verlag, pp. 132–142, 2009.

[37] K. Kitayama, Xu Wang, N. Wada, "OCDMA over WDM PON solution Path to Gigabit-Symmetric FTTH," J. Lightwave Technol., vol. 24, pp. 1654-1662, Apr. 2006.

[38] L. Galdino, T. R. Raddo, A. L. Sanches, L. H. Bonani, and E. Moschim, "Performance Comparison of Hybrid 1-D WDM/OCDMA and 2-D OCDMA Towards Future Access

Network Migration Scenario" in IEEE International Conference on Transparent Optical Networks, ICTON 2012, Coventry, England, July 2012.

[39] X. Wang, N. Wada, T. Hamanaka, T. Miyazaki, G. Cincotti, K. Kitayama, "OCDMA over WDM Transmission," in Proc. ICTON 2007, Rome, Italy, paper Tu.B1.1, July 2007.

[40] N. Ahmed, S. A. Aljunid, A. Fadil, R. B. Ahmad, M. A. Rashid, "Hybrid OCDMA/WDM system using complementary detection technique for FTTH access networks," 2011 IEEE Symposium on Industrial Electronics and Applications (ISIEA2011), Langkawi, Malaysia, pp. 237-230, Sept. 2011.

[41] Y. Cao, C. Gan, "A scalable hybrid WDM/OCDMA-PON based on wavelength-locked RSOA technology," Optik - International Journal for Light and Electron Optics, vol. 123, issue 2, pp. 176–180, July 2011.

[42] L. Yang, H. Zhang, X. Zheng, B. Zhou, Y. Guo, H. Wen, "Next Generation Hybrid OCDMA-WDM-PON with Soft Capacity," 15th OptoElectronics and Communications Conference (OECC2010) Technical Digest, Sapporo Convention Center, Japan, pp. 732-733, July 2010.

[43] R. A. Griffin, D. D. Sampson, and D. A. Jackson, "Coherence coding for photonic code-division multiple access networks," J. Lightwave Technol., vol. 13, pp. 1826–1837, Sept. 1995.

[44] M. E. Maric, "Coherent optical CDMA networks," J. Lightwave Technol., vol. 11, pp. 854–864, May 1993.

[45] H. Fathallah, L. A. Rusch, and S. LaRochelle, "Passive Optical Fast Frequency-Hop CDMA Communications System," IEEE J. Lightwave Technol., vol. 17, no. 3, pp. 397-405, Mar. 1999.

[46] M. Y. Azizoglu, J. A. Salehi, and Y. Li, "Optical CDMA via temporal codes," IEEE Trans. Commun., vol. 40, no. 7, pp. 1162-1170, Jul. 1992.

[47] B. M. Ghaffari and J. A. Salehi, "Multiclass, multistage, and multilevel fiber-optic CDMA signaling techniques based on advanced binary optical logic gate elements," IEEE Trans. Commun., vol. 57, no. 5, pp.1424-1432, 2009.

[48] E. K. H. Ng and E. H. Sargent, "Optimum threshold detection in realtime scalable high-speed multi-wavelength optical code-division multiple access LANs," IEEE Trans. Commun., vol. 50, no. 5, pp. 778–784, May 2002.

[49] S. Sahuguede, A. J.-Vergonjanne, and J.-P. Cances, "Performance of OCDMA system with FEC based on interference statistical distribution analysis," Eur. Trans. Telecomm., 21: 276–287. doi: 10.1002/ett.1387, Oct. 2009.

[50] A. L. Sanches, J. V. dos Reis, Jr., and B.-H. V. Borges, "Analysis of High-Speed Optical Wavelength/Time CDMA Networks Using Pulse-Position Modulation and

Forward Error Correction Techniques," IEEE J. Lightwave Technol., vol.27, no. 22, pp. 5134-5144, Nov. 2009.

[51] A. L. Sanches, "Análise de redes ópticas de alta velocidade baseadas na tecnologia CDMA e códigos bidimensionais (comprimento de onda/tempo)," Dissertation submitted for the degree of Master of Science at University of São Paulo (USP), São Carlos School of Engineering, 2010 (in Portuguese).

[52] N. G. Tarhuni and T. O. Korhonen, "Multi-weight multi-length strict optical orthogonal codes," in Proc. 6th Nordic Signal Processing Symp. (NORSIG), Espoo, Finland, Jun. 9–11, pp. 161–164, 2004.

[53] E. Inaty, H. M. H. Shalaby, P. Fortier, and L. A. Rusch, "Multirate optical fast frequency hopping CDMA system using power control," IEEE J. Lightwave Technol., vol. 20, no. 2, pp. 166–177, Feb. 2002.

[54] W. C. Kwong, P. Perrier, and P. Prucnal, "Performance comparison of asynchronous and synchronous code-division multiple-access techniques for fiber-optic local area networks," IEEE Trans. Commun., vol. 39, pp. 1625–1634, Nov. 1991.

[55] C. K. See, Z. F. Ghassemlooy, J. M. Holding, and R. McLaughlin, "Comparison of binomial and Gaussian distributions for evaluating optical DSCDMA system BER performance," in Proc. PREP, pp. 13-14, 2003.

[56] L. Nguyen, J. F. Young, and B. Aazhang, "Photoelectric current distribution and bit error rate in optical communication systems using a superfluorescent fiber source," J. Lightwave Technol., vol. 14, no. 6, pp. 1455–1466, Jun. 1996.

[57] K. Letaif, "The performance of optical fiber direct sequence spread spectrum multiple-access communication systems," IEEE Trans. Commun., vol. 43, pp. 2662–2667, Nov. 1995.

[58] N. G. Tarhuni, T. O. Korhonen, E. Mutafungwa, and M. S. Elmusrati, "Multiclass Optical Orthogonal Codes for Multiservice Optical CDMA Networks," IEEE J. Lightwave Technol., vol. 24, no. 2, pp. 694-794, Feb. 2006.

[59] S. V. Maric and V. K. Lau, "Multirate fiber-optic CDMA: System design and performance analysis," J. Lightwave Technol., vol. 16, no. 1, pp. 9–17, Jan. 1998.

[60] T. Miyazawa and I. Sasase, "Multi-rate and multi-quality transmission scheme using adaptive overlapping pulse-position modulator and power controller in optical network," in Proc. IEEE ICON, vol. 1, pp. 127–131, Nov. 2004.

[61] E. Inaty, P. Fortier, and L. A. Rusch, "SIR performance evaluation of a multirate OFFH-CDMA system," IEEE Commun. Lett., vol. 5, no. 5, pp. 224–226, May 2001.

[62] V. Eramo, "Impact of the MAI and beat noise on the performance of OCDM/WDM Optical Packet Switches using Gold codes," Opt. Express vol. 18, no. 17, pp. 17897-17912, 2010.

[63] N. Karafolas and D. Uttamcandani, “Optical fiber code division multiple access networks: A review,” Optical Fiber Technol., vol. 2, pp. 149–168, 1996.

[64] P. R. Prucnal, M. A. Santoro and T. R. Fan, “Spread Spectrum Fiber-optic Local Area Network Using Optical Processing,” J. Lightwave Technol., vol. LT-4, no. 5, pp. 547-554, May 1986.

[65] F. Coppinger, C. K. Madsen and B. Jalali, “Photonic Microwave Filtering Using Coherently Coupled Integrated Ring Resonators,” Microwave and Opt. Technol. Lett., vol. 21, No. 2, pp. 90-93, Apr. 1999.

[66] J. G. Zhang, Y. Wen, and P. Li, “Proposed OCDMA Encoders And Decoders Based Silica-On-Silicon Integrated Optics,” Microwave and Opt. Technol. Lett., vol. 40, no. 3,pp. 205-209, Feb. 2004.

[67] A. A. Shaar and P. A. Davies, “Prime Sequences: Quasi-Optimal Sequences for Channel Code Division Multiplexing,” IEEE Elect. Lett., vol. 19, no. 21, pp. 888-889, Oct. 1983.

[68] D. Zaccarin and M. Kavehrad, “An Optical CDMA System Based on Spectral Encoding of LED,” IEEE Phot. Techn. Lett., vol. 4, no. 4, pp. 479-482, Apr. 1993.

[69] M. Kavehrad and D. Zaccarin, “Optical Code-Division-Multiplexed Systems Based on Spectral Encoding of Noncoherent Sources,” J. Lightwave Technol., Vol. 13, No. 3, pp.534-545, Mar. 1995.

[70] M. Rochette, S. Ayotte, and L. A. Rusch, “Analysis of the spectral efficiency of frequency-encoded OCDMA systems with incoherent sources,” J. Lightwave Technol., vol. 23, no. 4, pp. 1610–1619, Apr. 2005.

[71] L. Tancevski and I. Andonovic, “Wavelength Hopping/Time Spreading Code Division Multiple Access Systems,” IEEE Electron. Lett., vol. 30, No. 17, pp. 1388-1390, Aug. 1994.

[72] L. Tancevski and I. Andonovic, “Hybrid wavelength hopping/time spreading schemes for use in massive optical networks with increased security,” J. Lightwave Technol., vol.14, no. 12, pp. 2636-2647, Dec. 1996.

[73] S. Shurong, H. Yin, and Z. Wang, “A new family of 2-D optical orthogonal codes and analysis of its performance in optical CDMA access networks,” J. Lightwave Technol., vol. 24, no. 4, pp. 1646-1652, Apr. 2006.

[74] L. Tancevski , M. Tur , J. Budin and I. Andonovic, “Hybrid wavelength hopping/time spreading code division multiple access systems,” Proc. Inst. Electr. Eng. Optoelectronics, vol. 143, pp. 161-166, Jun. 1996.

[75] S. P. Wan and Y. Hu, “Two-dimensional optical CDMA differential system with prime/OOC codes,” IEEE Photon. Technol. Lett., vol. 13, pp. 1373–1375, Dec. 2001.

[76] G. C. Yang and W. C. Kwong, “Performance comparison of multiwavelength CDMA and WDMA+CDMA for fiber-optic networks,” IEEE Trans. Commun., vol. 45, no. 11, pp. 1426-1434, Nov. 1997.

[77] K. O. Hill, G. Meltz, “Fiber Bragg Grating Technology Fundamentals and Overview,” IEEE Journal of Lightwave Technology, vol. 15, no. 8, pp. 1263-1276, July 1997.

[78] H. Fathallah, “Optical fast frequency hopping CDMA: principle, simulation and experiment,” Thesis submitted to the degree of doctor philosophy at Universitè Laval, Facultè Des Sciences et de Gènie, 2002.

[79] E. Inaty, H. M. H. Shalaby, and P. Fortier, “On the cutoff rate of a multiclass OFFH-CDMA system,” IEEE Trans. Commun., vol. 53, no. 2, pp. 323–334, Feb. 2005.

[80] L. Bin, “One-Coincidence Sequences with Specified Distance Between Adjacent Symbols for Frequency-Hopping Multiple Access,” IEEE Transactions on Communications, vol. 45, no. 4, pp. 408-410, April 1997.

[81] A. A. Shaar and P. Davies, “A survey of one coincidence sequences for frequency-hopped spread spectrum systems,” Inst. Elect. Eng. Proc., vol. 131, no. 7, pp. 719–724, Apr. 1984.

[82] E. Inaty, L. A. Rusch, and P. Fortier, “Multirate optical fast frequency hopping CDMA system using power control,” in IEEE Globecom 2000, vol. 2, San Francisco, CA, pp. 1221–1228, Nov. 2000.

[83] J. Mendez, R. M. Gagliardi, V. J. Hernandez, C. V. Bennett, and W. J. Lennon, “High performance optical CDMA system based on 2-D optical orthogonal codes,” J. Lightwave Technol., vol. 22, no. 11, pp. 2409–2419, 2004.

[84] T. R. Raddo, A. L. Sanches, J. V. dos Reis, Jr., and B.-H. V. Borges, “A New Approach for Evaluating the BER of a Multirate, Multiclass OFFH-CDMA System,” IEEE Communications Letters, vol. 16, no. 2, pp. 259-261, Feb. 2012.

[85] H. Lundqvist and G. Karlsson, “On error-correction coding for CDMA PON,” IEEE J. Lightwave Technol., vol. 23, no. 8, pp. 2342–2351, Aug. 2005.

[86] D. C. Montgomery and G. C. Runger, Applied Statistic And Probability For Engineers, 3rd ed., Ed. John Wiley & Sons, Inc., pp. 119, 2002.

[87] H. Sotobayashi, W. Chujo, and K. Kitayama, “Transparent virtual optical code/wavelength path network,” IEEE J. Select. Topics Quantum Electron., vol. 8, pp. 699–704, May/June 2002.

[88] K. Kitayama, H. Sotobayashi, and N. Wada, “Optical code division multiplexing (OCDM) and its application to photonic networks,” IEICE Trans. Fund. Electron., Commun. Comput. Sci., vol. E82-A, no. 12, pp. 2616–2626, 1999.

[89] F. R. Durand, F. R. Barbosa, and E. Moschim, “Performance analysis of optical code switching router,” European Transactions on Telecommunications, vol. 21, pp.101–107, 2010.

[90] H. Sotobayashi, W. Chujo, and K. Kitayama, “Highly spectral efficient optical code division multiplexing transmission system,” IEEE J. Sel. Topics Quantum Electron., vol. 10, no. 2, pp. 250–258, Mar./Apr. 2004.

[91] K. Kitayama, “Code Division Multiplexing Lightwave Networks Based upon Optical Code Conversion,” IEEE J. Sel. Areas Comm., no. 16, pp. 1309–1319, 2000.

[92] T. R. Raddo, A. L. Sanches; J. V. dos Reis Jr. and B.-H. V. Borges, “Performance evaluation of a multirate, multiclass OCDM/WDM optical packet switch,” Microwave & Optoelectronics Conference (IMOC), 2011 SBMO/IEEE MTT-S International, vol., no., pp. 824-828, Oct. 2011.

[93] V. Eramo, “An Analytical Model for TOWC Dimensioning in a Multifiber Optical-Packet Switch,” J. Lightwave Technol., vol. 24, no. 12, pp. 4799-4810, 2006.

[94] G. E. P. Box, J. S. Hunter, and W. G. Hunter, Statistics for experimenters: Design, Innovation, and Discovery, 2nd ed., Wiley-Interscience, 2005.